Catena 214 (2022) 106259

Contents lists available at ScienceDirect

Catena

journal homepage: www.elsevier.com/locate/catena

Effects of gully control measures on sediment yield and connectivity in wooded rangelands

Alberto Alfonso-Torreño [a,*], Susanne Schnabel [a], Álvaro Gómez-Gutiérrez [a], Stefano Crema [b], Marco Cavalli [b]

[a] Research Institute for Sustainable Land Development (INTERRA), University of Extremadura, Cáceres, Spain
[b] National Council of Research, Research Institute for Geo-Hydrological Protection, Padova, Italy

ARTICLE INFO

Keywords:
Valley-bottom gully
Sediment load
Control measures
Sediment connectivity
Multi-temporal DEMs

ABSTRACT

Gully rehabilitation is often applied as part of catchment management strategies aimed at reducing downstream sediment yields. However, the influences of gully control measures on the runoff and sediment transport processes in agroforestry systems have been seldom studied. In this paper, a thorough analysis of these processes was carried out in a valley-bottom gully located in a dehesa from SW Spain. The gully was monitored before and after implementation of different runoff and sediment control measures that included: gabion check-dams, brushwood check-dams and livestock exclusion through fencing. The aims of this work are: (1) to analyze the effect of the gully control measures on the hydrological dynamics and sediment load, and (2) to evaluate their effect on sediment connectivity at the catchment and channel scales. Changes in topography and connectivity were estimated using sequential Digital Elevation Models (DEMs) with a resolution of 0.02 m generated by Structure – from – Motion photogrammetry from aerial images acquired by an Unmanned Aerial Vehicle. Discharge and suspended sediment were monitored at the outlet. Results indicate that flood discharge was not influenced by the control measures, but suspended sediment concentration was reduced by 65%. The integration of the difference of connectivity index with topographic change maps highlighted the impact of the gully control measures on changes in sediment connectivity. A strong relationship between geomorphic dynamics and the spatial pattern of hydrological and sediment pathways were observed in the gully. The connectivity index (IC) increased in eroded areas, while deposition sites showed a decrease in the IC. Connectivity also decreased in the bank headcuts located within an area isolated from livestock. The implementation of runoff and sediment control measures in the channel was successful in stabilizing the expansion of the channel network and had beneficial effects in the short-term but further monitoring would be necessary to understand long-term effects.

1. Introduction

Soil erosion is one of the main factors leading to land degradation worldwide, being water erosion the dominant process (Bakker et al., 2004; Boardman et al., 2003; Zhao et al., 2019). The Mediterranean region is prone to soil erosion by water due to intense rainfall events and long-lasting droughts, steep slopes combined with complex and rough terrain and human activity reflected in the recurrent use of fire, farming and overgrazing (García-Ruiz et al., 2013). In the southwestern part of the Iberian Peninsula, a wooded rangeland with an agro-silvopastoral land use system, named *dehesa*, covers >4 million ha (Fig. S1). Although the largest extension is found in the southwestern part of the Iberian Peninsula, there are similar agroforestry systems in the whole Mediterranean region (e.g. In Portugal: Pinto-Correia et al., 2011; in Greece: Kizos and Plieninger, 2008). It is formed by cleared oak woodlands with an annual grassland understory that is grazed by cows, sheep, pigs and horses (Eichhorn et al., 2006). The sustainability of the dehesa ecosystem is threatened by deforestation, overgrazing and land use changes (Herguido Sevillano et al., 2017; Pulido et al., 2018) which contribute to the generation of runoff and sediment yield. Soil erosion by water promotes a decrease in the amount of water and soil and impacts on water reservoirs causing a loss of productivity (Schnabel et al., 2010). Soils in dehesas are commonly shallow, except for the valley bottoms where they are deeper. Infiltration capacity of the soils on hillslopes is low, provoking rapid runoff generation in the channel (Cerdà et al., 1998; Ceballos and Schnabel, 1998).

* Corresponding author.
E-mail address: albertoalfonso@unex.es (A. Alfonso-Torreño).

https://doi.org/10.1016/j.catena.2022.106259
Received 17 July 2021; Received in revised form 8 March 2022; Accepted 27 March 2022
Available online 2 April 2022

In dehesas, soil erosion by water was studied in two small experimental catchments with similar topographical and environmental conditions: Guadalperalón (Schnabel et al., 2010) and Parapuños (Alfonso-Torreño et al., 2021; Gutiérrez et al., 2009; Schnabel et al., 2013), being the latter the study area of the present research. The Parapuños experimental catchment can be considered a model of the dehesa exploitation system for its representativeness in terms of land use and management. At the same time, the existence of previous research sets the basis for a medium-term analysis of the hydrological and sedimentological behavior of the catchment and for the investigation of hillslope-to-channel runoff and sediment connectivity. Channel flow in these small catchments is highly variable in time and depends largely on the rainstorm intensity-duration characteristics, the antecedent moisture conditions and especially on the water content of soils in the valley bottoms (Ceballos and Schnabel, 1997; Schnabel and Gómez-Gutiérrez, 2013). Hortonian type overland flow dominates under dry soil conditions and is produced by high intensity rainfall, whereas saturation excess flow and preferential subsurface flow processes occur with humid antecedent conditions and are responsible of most of the runoff generated (Schnabel and Gómez-Gutiérrez, 2013; Schnabel et al., 2018). Sheetwash, the dominant erosion process at hillslopes was estimated to be 0.63 t ha^{-1} y^{-1} in a similar catchment using open plots, but with smaller stocking rates (Schnabel, 1997; Schnabel et al., 2010). Gully erosion is observed in the valley-bottoms and produced an average loss that varied from 0.07 t ha^{-1} y^{-1} (Gómez-Gutiérrez et al., 2012) to 1.55 t ha^{-1} y^{-1} (Schnabel et al., 2010). More recent studies in dehesas estimated soil erosion rates in the order of 18.5 t ha^{-1} y^{-1} from 1881 to 2014 (Rubio-Delgado et al., 2017; Rubio-Delgado et al., 2018), using exposed tree roots and ^{137}Cs. However, there is a lack of information regarding the relationship between gully erosion and catchment hydrology, mainly due to the difficulties to carry out a continuous and long term monitoring of topographic channel changes, rainfall and discharge (Gómez-Gutiérrez et al., 2012). Summarizing, previous studies quantified soil erosion rates, studied the causes and factors that encouraged soil erosion and highlighted the problem of soil degradation by water erosion in dehesas. Gully erosion drives the overland flow and causes a significant loss of runoff, decreasing soil moisture and consequently reducing grassland availability for livestock.

In order to restore degraded areas affected by gullying, different strategies have been applied (Frankl et al., 2021; Heede, 1978; Pathak et al., 2005). According to Frankl et al. (2021), runoff and sediment control measures may be conducted at different spatial scales, and can be grouped as follows: (1) treating the catchment with measures including livestock control, soil bunds (i.e., embankment), infiltration ditches and revegetation or water-retention measures such as ponds; (2) installing devices in the gully such as sediment traps, check dams, rockfills or breakwaters; (3) implementing actions taken adjacent to the gully such as livestock exclosure by fencing to avoid the mechanical effect of animal movement; and (4) applying a combination of all three approaches (Bartley et al., 2020). In Mediterranean areas, check dams are often used, sometimes in combination with other measures to retain sediments (Alfonso-Torreño et al., 2019; Castillo et al., 2007), to decrease catchment sediment yield (Quiñonero-Rubio et al., 2016) and to control sediment transport after wildfires (González-Romero et al., 2021). Nevertheless, only a few soil engineering and bioengineering structural measures have been implemented in the dehesa ecosystem and evaluation of the effectiveness of those measures is nearly absent. A recent exception is the work by Alfonso-Torreño et al. (2019) who calculated the sediment volume deposited behind 160 check dams in a dehesa in SW Spain. Results showed a high spatial variability in sediment deposition, with largest volumes of material accumulated in the lower areas of the catchment whereas the upper parts featuring a lower degree of sediment connectivity showed lower deposition volumes. In a recent study, Alfonso-Torreño et al. (2021) found that the gully control measures implemented in the Parapuños channel favored stabilization of the gully, favoring sediment deposition and reducing the slope of the channel bed. On the one hand, there is growing attention in the literature about the role of channel control measures on changes in sediment connectivity (e.g., Cucchiaro et al., 2019; Marchi et al., 2019), on the other hand, there are some important gaps of knowledge about the effect of the check dams on the discharge and the suspended sediment in semiarid silvopastoral systems. This research subject has already been studied in other ecosystems. For instance, check dams probed to be suitable to trap sediments (Belmonte et al., 2005; Conesa García, 2004), avoiding transfer of sediments downstream of the check dam (Conesa García, 2004; Martín-Rosales et al., 2003) and reducing sediment yields (Castillo et al., 2007; Heede, 1978; Polyakov et al., 2014). It is well documented that check dams typically have a limited life span and their effectiveness generally decreases over time as these hydraulic structures fill with sediment (Gifford et al., 1977; Taye et al., 2015). However, Tang et al. (2020) demonstrated in a small catchment (4.26 km^2) in the Loess Plateau that filled check dams were still able to reduce flood peaks by 31% to 93%.

In the last decades, improvements in remote sensing techniques (e.g., LiDAR and SfM-MVS) and platforms (e.g., UAVs) have greatly improved our capacity to understand factors and processes driving gully erosion (Koci et al., 2020; Sidle et al., 2019). These advances have also opened up hopeful opportunities for the study of geomorphological processes focused on hydrological and sediment connectivity (e.g., Cavalli et al., 2019; Heckmann et al., 2018). The concurrent use of UAV platforms and SfM-MVS has meant a breakthrough in acquiring very high resolution (centimeter) topographic data and in 3D model generation. Repeated high-resolution digital elevation models are key to identify overland flow and sediment pathways (Heckmann and Vericat, 2018), to detect geomorphic changes (Alfonso-Torreño et al., 2021; Cavalli et al., 2017; Turner et al., 2015; Woodget et al., 2015) and to analyze structural and functional connectivity changes (Cucchiaro et al., 2019).

The concept of sediment and hydrological 'connectivity' supplies a valuable tool for the analysis of the linkage between pathways and overland flow in hillslopes and the dynamics of erosion and deposition in valley-bottom gullies. In general terms, hydrological and sediment connectivity describes the degree to which a system facilitates water and sediment transfer through coupling relationships among its different components (Bracken and Croke, 2007; Heckmann and Vericat, 2018; Koci et al., 2020; Sidle et al., 2017). Connectivity can be expressed in terms of lateral (i.e. hillslope-to-channel) and longitudinal (i.e. along the channel network) coupling (Brierley et al., 2006; Fryirs et al., 2007). According to Lehotský et al. (2018), there is a large gap between studies undertaken on hillslope processes and those in channel environments. Gullies are influenced by hillslope and channel processes, which provide an outstanding chance to link and study both topographic positions.

Erosion and deposition dynamics in a channel reflect, to a certain extent, the capacity of that channel (or reach) to retain or export sediment (i.e., sediment connectivity) (Wohl et al., 2017). Studies focused on this subject point out that connectivity can fluctuate in a system (Heckmann and Vericat, 2018). This variability may be related to the spatial pattern of hydrological and sediment pathways and shows the capacity of the different landscape features to be linked (i.e., structural connectivity) (Cavalli et al., 2013). The concept of 'connectivity' may also be related to the actual sediment transfer between the components of a geomorphological system at a specific location and time (i.e., functional connectivity) (Bracken et al., 2015). In this context, the volume of sediments entrained along a channel or retained behind a check-dam can be considered a measure of functional sediment connectivity and, at the same time, plays an important role in disconnectivity acting as a barrier (Bracken et al., 2015; Fryirs et al., 2007). The potential of a landscape to be connected has been widely analyzed applying sediment connectivity indices (Borselli et al., 2008; Cavalli et al., 2013; Heckmann and Vericat, 2018; Quiñonero-Rubio et al., 2013). The topographically based index of sediment connectivity (IC), aimed at characterizing connectivity patterns at the catchment scale providing an estimation of the potential connection of sediment sources and a definition of

sediment transfer paths (Cavalli et al., 2020), was originally proposed by Borselli et al. (2008) for application in cropland catchments. IC was later modified by Cavalli et al. (2013) for better exploiting high-resolution DEMs. The IC has been widely used, for example by López-Vicente et al. (2013) and López-Vicente et al. (2017) who analyzed the effects of land uses and land abandonment on sediment connectivity changes in Mediterranean mountain catchments. Quiñonero-Rubio et al. (2013) identified where check dams had a huge impact on sediment (dis)connectivity in a Mediterranean catchment applying the Catchment Connectivity Index (CCI). Although the IC by Cavalli et al. (2013) was developed in mountainous environments, it could potentially be used to analyze the spatial connectivity patterns in lower slope gradient catchments and thus determine the degree of connection between different locations in a watershed to receive and export flow and sediments. In addition, the connectivity between hillslopes and valley-bottoms allows the identification of intersection points between runoff and sediment flow pathways and the filled areas in a gully.

The present work aims to analyze the effect of runoff and sediment control measures in a small semiarid rangeland catchment. The runoff and sediment control measures implemented in the valley bottom gully were gabion check dams, brushwood check dams and livestock fencing. Furthermore, the following secondary objectives are included: (1) to analyze the effect of the gully control measures on the hydrological dynamics and suspended sediment yield, and (2) to evaluate their effect on storage and sediment connectivity at the catchment and channel scales.

2. Study area

The present work was carried out in Parapuños, an experimental catchment (99.5 ha) located in SW Spain (Fig. 1a). Parapuños is a typical Mediterranean rangeland with a dehesa land use system, characterized by a disperse tree cover of Holm oak (*Quercus ilex va. rotundifolia*), with an average tree density of 22.5 trees ha^{-1}, and herbaceous plants in the understory (Fig. 2). At steeper slopes shrubs are frequent, mainly composed of *Retama sphaerocarpa*, *Cytisus multiflorus* and *Genista hirsuta*. The farm is grazed by approximately 1,000 sheep, 55 cows and 40 pigs. Historically, dehesas have experienced important land use and vegetation cover changes, specifically, in the study area these changes have been related to soil erosion processes (Gutiérrez et al., 2009; Rubio-Delgado et al., 2018).

The study basin has an average elevation of 396 m above sea-level, ranging from 362 to 434 m and an average slope of 8%. SSW is the dominant aspect within the catchment. There are two types of bedrock in the catchment: Ediacarian slates and unconsolidated conglomerates (Miocene), forming part of remnants of a pediment that occupy 32% of the catchment. This pediment is composed of quartzite cobbles, gravelly sand and a clay-rich layer at approximately 0.5 m depth. The major portion of the pediment is located in the northern part of the basin and a small remnant is found in the SE, forming a hill. The main pediment can be divided into a flat upper surface and a slope with gradients close to 25% (Fig. 1). The valley-bottom (i.e., the alluvial sediment fill) is an undulating area with a slope <5%.

The soils within the catchment are commonly shallow and classified as Leptosols and Cambisols at hillslopes and Regosols at valley bottoms. The alluvial sediment fill, where the gully is located, are Regosols and are acid, with a pH ranging between 4.7 and 6.4, a low organic matter content (1.4%) and a low cationic exchange capacity (<6 meq 100 g^{-1}). The pediment area shows a high content of rock fragments (32%), whereas silt and sand were the dominant fractions of soils on the lower slopes developed on slates (44% and 39%, respectively). Soils in valley bottom are also formed on slates with 53 and 11% of silt and clay, respectively, and the lowest proportion of sand. In contrast to the valley bottoms, the channel banks have a higher content of sand and coarse

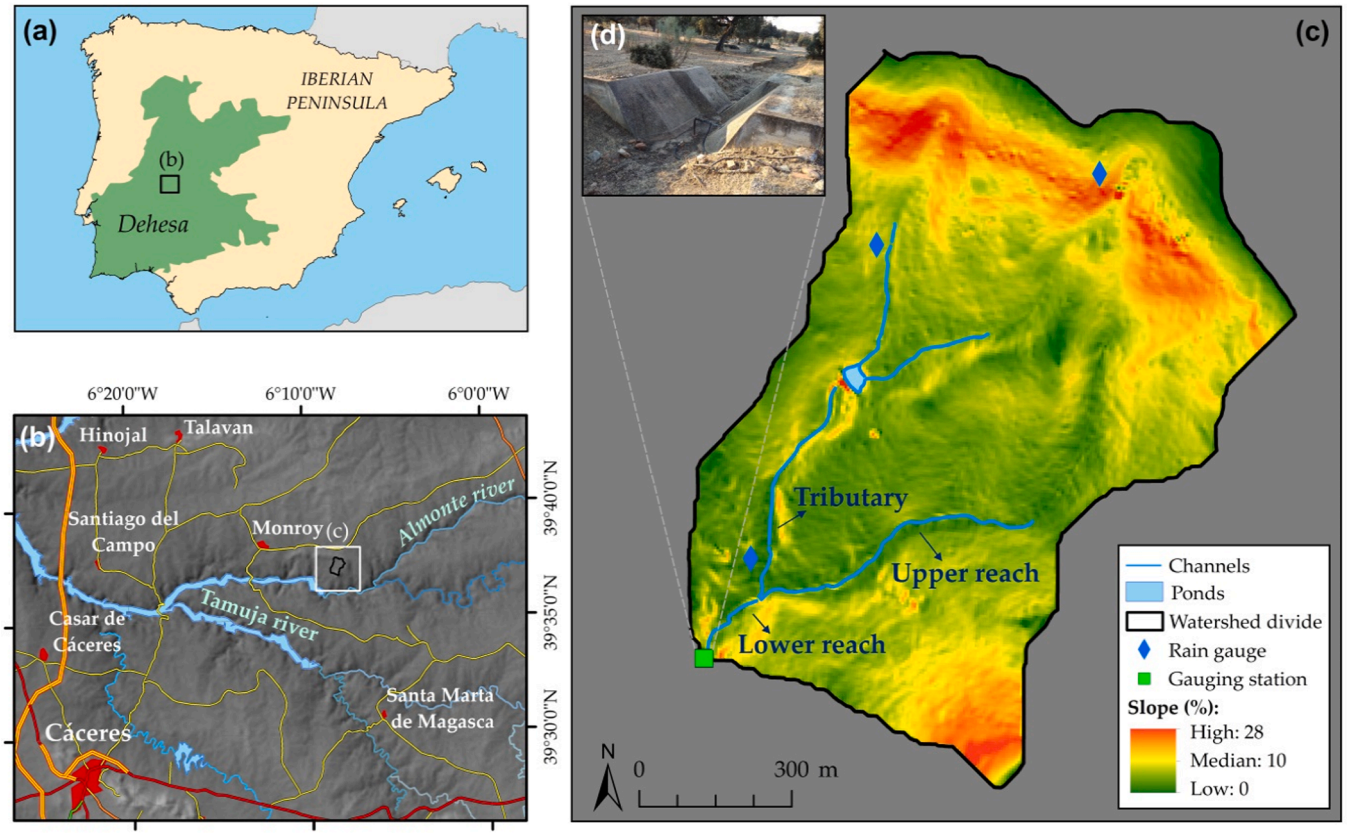

Fig. 1. (a) Spatial distribution of dehesa landscapes in the SW of the Iberian Peninsula, (b) regional setting of the studied catchment, (c) Parapuños catchment including slope gradient, the equipment, and the channel reaches and (d) a gauging station at the catchment outlet.

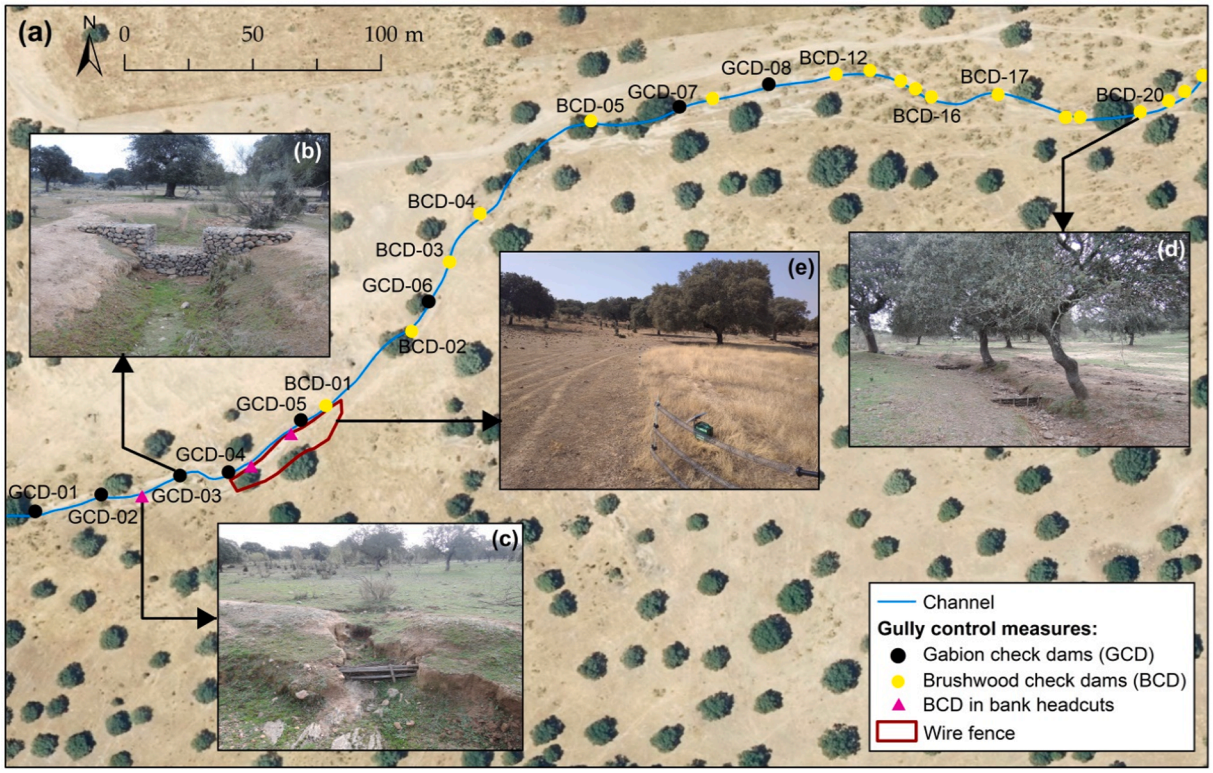

Fig. 2. (a) Location of the gully control measures (i.e., gabion check dams (GCD), brushwood check dams (BCD) and a wire fence) and (b-e) examples of soil engineering and bioengineering structural measures implemented in the upper reach: (b) a GCD, (c) a BCD in a bank headcut, (d) a BCD in the channel, and (e) the isolated area by a fence in the left bank of the gully.

elements (32% and 24%, respectively).

Climate is Mediterranean with an average annual temperature of 16 °C and a mean annual rainfall of 513 mm with high seasonality and absence of snowfall. The rainy season ranges from October until April, being October the rainiest month with 83.0 mm on average. The summers are hot and dry, with July and August registering very low amounts of rainfall. Interannual rainfall variability is high with annual totals that ranged from 292 to 802 mm for the period 2000 to 2018. Rainfall and discharge data are calculated for hydrological years from September to October. Maximum flood discharge totals were registered in February and March and minimum values from June to September. Temporal variability of discharge is even more pronounced than that of rainfall, being the coefficients of variation 109% and 30%, respectively.

The gully has been previously defined as a valley bottom gully (Gutiérrez et al., 2009) and constitutes a discontinuous second-order stream composed of the main channel and a tributary, with a length of 832 m and 163 m, respectively (Fig. 1c). The channel is situated in the lower part of the watershed and is incised into the alluvial sediment fill with an approximate depth of 1.5 m, reaching even the underlying schist at some sites. The gully may be divided into three different reaches: (1) lower reach, (2) tributary reach and (3) upper reach where the soil engineering and bioengineering structural measures were carried out in February 2017 (Fig. 1c). The lower reach connects the junction between the tributary and the upper reach with the outlet of the catchment.

Eight gabion check dams (GCDs) with metal mesh and 25 brushwood check dams (BCDs) were built in the channel in February 2017 (Fig. 2a) with the aim of trapping sediments and reducing lateral bank erosion. The GCDs have a width of 0.5 m with lengths between 1 and 3 m and most of them a height of 1.5 m. They have a central spillway (Fig. 2b) and are located with an average separation of 27 m. The mesh was manually filled with quartzite cobbles collected in the area. BCDs were made with brooms growing in the area, anchored to the surface with acacia posts, a rot-proof wood, and tied with hemp material (Fig. 2d). The BCDs have a length of 2 m and a mean separation of 12 m. BCDs were also installed at three bank headcuts (Fig. 2c). Finally, a wire fence was set up adjacent to the gully as a livestock exclusion measure implemented in a particularly degraded area that showed several active bank headcuts. The wire fence has a perimeter of 117 m and isolates 416 m^2 (Fig. 2e).

3. Material and methods

3.1. Rainfall, discharge and suspended sediment measurements and sediment deposit sampling

The catchment is equipped with three tipping bucket rain gauges (model RG3, Onset Hobo) that record with a resolution of 0.2 mm and collect in a 5 min interval. Discharge and suspended sediment were measured at the outlet of the catchment in a weir formed by a V-notched section and a trapezoidal approximation reach (Fig. 1d). A capacitive sensor (Unidata 6521 l) was used to obtain water depth data with a range of discharge of 1–4000 l s^{-1} (Schnabel et al., 2013). Suspended sediment concentration was determined using a turbidity meter (OBS-3A). The water depth probe and the turbidimeter were connected to a datalogger (Datataker DT50) registering in 5-minute intervals. Furthermore, suspended sediment concentration was also obtained from water samples taken with an automatic pump sampler (model Isco 3700C) with 24 bottles of 0.5 l volume, installed in the gauging station and controlled by the datalogger. Water sampling takes place when water level exceeds 0.15 m, corresponding to a discharge of 10.4 l s^{-1}. The turbidity sensor was previously calibrated with a range of concentrations and is, as well, controlled by concentrations obtained from the ISCO samples (Fig. S2).

Grain size distribution of sediments deposited behind GCDs was determined. For this, sediment behind GCDs was sampled in 6 locations with an auger (Eijkelkamp). Samples were air dried and disaggregated.

The coarse fraction was determined by sieving and the grain size distribution of the fine fraction was carried out using a laser particle analyser (Beckman coulter) applying the USDA classification (USDA, 2004).

3.2. Hydrological data processing and analysis

Three different temporal scales were used for analyses: rainfall event, month and hydrological year. A database composed of events that produced runoff from September 2013 to 2019 was created. The database was grouped before (i.e. from September 2013 to February 2017) and after (i.e., from February 2017 to January 2019) implementation. The events were differentiated in time using a minimum interval between two consecutive events of one hour without precipitation. The same interval was also used by Lana-Renault et al. (2008) for another small Mediterranean catchment. In order to separate base flow from direct runoff (flood discharge) two methods were applied and compared: the straight line method with inclination (Chow et al., 1988) and the straight line method with a fixed gradient (Chow et al., 1988). Best results were obtained with the straight line method with inclination because this method produced a better adjustment for the flood hydrographs. The criteria used for defining the start of flood discharge was 1.5 times the amount of base flow (Lana-Renault et al., 2008). The technique of the normal depletion curve was applied for identifying the point that establishes the end of direct runoff in a hydrograph (Horton, 1933).

A total of 18 variables were derived from rainfall, discharge and sediment records at the event scale for carrying out the statistical analysis and defining relevant relationships amongst them (Table 1).

The values of runoff and sediment variables did not follow a normal frequency distribution and generally are positively skewed. The nonparametric Kolmogorov–Smirnov and Mann–Whitney test were used to test the significance of differences of rainfall, discharge and sediment variables grouped according to period, i.e., before (BEF) and after (AFT) gully control measure construction. Furthermore, Spearman's rho test was used to detect correlations between the variables". Spearman's correlation coefficients are used instead of Pearson's because most of the data are not normally distributed. All the tests were two-tailed, applying significance p-levels of 0.05 and 0.10. Regression analysis was conducted in order to describe the rainfall-flood relationships by grouping the rainfall events depending on antecedent catchment soil moisture conditions. Nonlinear regression models were used to establish correlations and the Levenberg-Marquardt algorithm was applied for estimating the parameters. Statistical analysis were conducted using STATISTICA© software.

3.3. 3D models acquisition, DoD elaboration and computation of hydrological connectivity

The DEM database used to describe geomorphic changes and to estimate the connectivity indices was elaborated for the previous work by Alfonso-Torreño et al. (2021) and hence only a brief description of the its elaboration is presented in the following. These authors estimated the geomorphic changes in the valley-bottom gully in the 2016 to 2019 time window, by using high-resolution DEMs produced through aerial images and SfM-MVS photogrammetric techniques. The dataset was taken in five different surveys using a fixed-wing UAV (Ebee classic by Sensefly) carrying a Sony WX220 sensor on board (18 Mpx). The images were acquired at an approximate altitude of 60 m above ground resulting in a Ground Sampling Distance of 2 cm. An average number of 190 images were captured per survey. The models were scaled and georeferenced using twenty Ground Control Points (GCPs) which were registered across the area and surveyed with the help of a Global Navigation Satellite system working in Real Time kinematic mode. The Pix4Dmapper Pro software (v. 3.1.18) was fed with the images and the GCPs in order used for the photogrammetric processing to produce 2.5D (Digital Surface Model or DSM, Digital Elevation Model or DEM and orthophotographs) and 3D cartographic products (point cloud). During the processing, a mean Root Mean Square Error of 0.03 m was estimated.

Topographic changes were estimated comparing the DEMs produced for each UAV survey and using the classical DoD (Wheaton et al., 2010). To do this, the Geomorphic Change Detection v7.1 add-in (Riverscapes-Consortium, 2018) freely available from https://gcd.joewheaton.org/downloads, within the ArcGIS Desktop software v10.6 was used. We considered a spatially variable error estimated using rules implemented through a fuzzy inference system (FIS) in addition to the georeferencing error calculated for every individual DEM during the photogrammetric processing. Two rules, based on slope gradient and vegetation height (i.e., wood vegetation and grasses), were used in the FIS system. The SfM-derived DEMs allowed the estimation of the geomorphic changes at the gully before (BEF) and after the gully control measures (AFT).

The IC formulated by Borselli et al. (2008), with the changes proposed by Cavalli et al. (2013), was used to evaluate the potential connection between the watershed slopes and the valley-bottom channel. This dimensionless index is expressed as the logarithm of the ratio of an upslope and downslope component, representing the potential for downward routing of the sediment produced upslope and the flow path length that a particle has to travel to arrive at the nearest target (i.e., the outlet of the catchment in this study. Both components consider a surface roughness index (i.e., the local topography variability) as the impedance to runoff and sediment fluxes. More details on the formula and the calculation can be found in Cavalli et al. (2013).

The IC was computed for the study basin by using SedInConnect 2.3 software (Crema and Cavalli, 2018), which includes the modifications proposed by Cavalli et al. (2013). The IC was calculated for each date (i.e., each UAV survey) using two merged DEMs. For the valley-bottom area, the SfM-derived DEM acquired at each date (0.1 m) was used while for the rest of the catchment a 5 m resolution DEM (Spanish National Geographic Institute) produced by LIDAR techniques was applied. Both DEMs were merged to a resampled DEM of 0.5 m pixel size and a moving window of 3x3 pixels was set for Manning's n roughness computation. The input DEM was hydrologically corrected using the Pit remove tool of the TauDEM 5.3.7 add-in (Tarboton et al., 2015) freely available from https://hydrology.usu.edu/taudem/taudem5/, within the ArcGIS Desktop software v10.5.

The changes of IC (DoIC) experienced during the study period were calculated by subtracting the 2019 IC map from the 2016 IC to investigate the influence of the gully control measures on sediment connectivity dynamics. Finally, we compared DoIC maps with the erosion and deposition patterns derived from the DoDs.

Sediment retention and sediment erosion were considered as measures of connectivity in the gully. Channel sediment disconnectivity may be defined as the ability of a certain channel reach to retain or deposit sediments (Hooke, 2003). Therefore, the amount of sediments deposited or retained along a channel reach (e.g., with the implementation of runoff and sediment control measures) is an estimation of sediment connectivity (or dis-connectivity) (Bracken et al., 2015; Fryirs, 2013; Wester et al., 2014; Wohl et al., 2017). Following this definition, Calle et al. (2020) applied a connectivity value for a defined channel reach or strip (Cv-strip). This connectivity value is calculated as the ratio of eroded material to the deposited sediments for a specific period (eq. (2)):

$$C_{v-strip} = \frac{Erosion}{Deposition} \quad (2)$$

This ratio involves more channel connectivity at eroded reaches with values of Cv-strip > 1. On the other hand, reaches that experienced deposition present Cv-strip < 1 and show, by definition less connectivity. In our study, the channel was divided into reaches of 5 m of length (i.e., less than the minimum distance between gully control measures), resulting in 88 strips.

4. Results

4.1. Characteristics of rainfall, discharge and sediment load

The average annual rainfall in the basin was 506 mm for the period 2013 to 2019. The annual sediment load was 73.8 tons on average, equivalent to 0.72 t ha^{-1} y^{-1}. The interannual variation was very high, ranging from 0.03 in 2014–15 to 1.39 t ha^{-1} y^{-1} in 2016–17, with a standard deviation of 0.56 t ha^{-1} y^{-1} (Fig. 3). Suspended sediment load>1 t ha^{-1} only took place when rainfall >450 mm was recorded. However, large discharge may also produce small amounts of sediment load.

As far as the event time scale is concerned, a total of 111 rainfall events were included in the data base which produced a median flood discharge of 118.4 m^3. Table S1 presents basic statistics of variables related to discharge, rainfall and suspended sediment. In the set of 111 events analyzed, only 80 events produced suspended sediment load, of which 53 were registered before gully control measure construction and 27 afterwards. The median event suspended sediment load was 0.1 t, being the lower and the upper quartile 0.0 t and 0.7 t. Mean event suspended sediment concentration showed a median of 0.2 g l^{-1} ranging from 0 to 3.4 g l^{-1}. Rainfall events that generated suspended sediment load only took place between September and April.

Median event rainfall was 10.3 mm, with lower and upper quartiles of 5.0 and 15.0 mm, respectively. A total of 48% of the rainfall events were of small magnitude (<10 mm) and did not present a clear seasonal pattern, i.e., they are equally frequent at any time of the year, except for July and August. The 5-minute maximum rainfall intensity had a median of 10.5 mm h^{-1} and 25% of the events registered<7.2 mm h^{-1}. The maximum 60-minute rainfall intensity ranged between 1 mm h^{-1} and 19.0 mm h^{-1}, with only 10% of the sample above 9.6 mm h^{-1}.

Although the relationship between rainfall and flood discharge is significant ($p < 0.05$), the correlation coefficient R is low for the entire dataset (Table 2). Flood discharge and maximum flood discharge correlated significantly with rainfall intensity in 60 min, amount of rainfall recorded 10, 20 and 40 days before the event and maximum peak flow. Maximum suspended sediment concentration correlated significantly and positively with rainfall intensity in 5 min, sediment load and mean suspended sediment concentration. However, no relationship could be detected with the amount of rainfall recorded prior to the event (Table 1) and discharge. Mean suspended sediment concentration correlated significantly and positively with maximum peak flow, sediment load and maximum suspended sediment concentration.

Table 1
Rainfall, discharge and suspended sediment variables, showing the corresponding abbreviations and measuring units.

Type of variable	Abbreviation	Units	Description
Rainfall	*R*	mm	Total amount of event rainfall
	I5, I10, I30 and I60	mm h^{-1}	Maximum rainfall intensities in 5, 10, 30 and 60 min
	D1, D5, D10, D20 and D40	mm	Amount of rainfall recorded 1, 5, 10, 20 and 40 days prior to the event
Discharge	*Q_max*	l s^{-1}	maximum peak flow
	Discharge	m^3	Total discharge
	Flood discharge	m^3	Total amount of event runoff
	Discharge base flow	m^3	Total amount of base flow during the flood runoff
	Runoff coefficient	%	A dimensionless coefficient relating the amount of runoff to the amount of rainfall received
Sediment transport	*Suspended sediment load*	t	Amount of suspended sediments at the outlet of the catchment
	Max concentration	g l^{-1}	Maximum suspended sediment concentration
	Mean concentration	g l^{-1}	Mean suspended sediment concentration

Nevertheless, no relationship could be detected with rainfall variables. Suspended sediment load obtained a stronger correlation with mean suspended sediment concentration than with maximum sediment concentration.

The relationship between rainfall and runoff improved by grouping the rainfall events, resulting in three groups that express different antecedent catchment soil moisture conditions: Dry, Intermediate and Humid. Table S2 shows the regression equations for the three groups and the corresponding statistical parameters. All events with a base flow > 0.07 l s^{-1} and with 150 mm of antecedent rain (RAnt) or mean accumulated rainfall (M_RAnt) > 2.0 mm were classified as Humid. Intermediate events are those with a base flow > 0.07 l s^{-1}, RAnt > 150 mm and M_RAnt < 2.0 mm. Dry events are those with RAnt < 150 mm. The non-parametric Kolmogorov-Smirnov test showed that group Dry was significantly different from group Humid and Intermediate ($p < 0.05$), although the humid events were not significantly different from the intermediate ones.

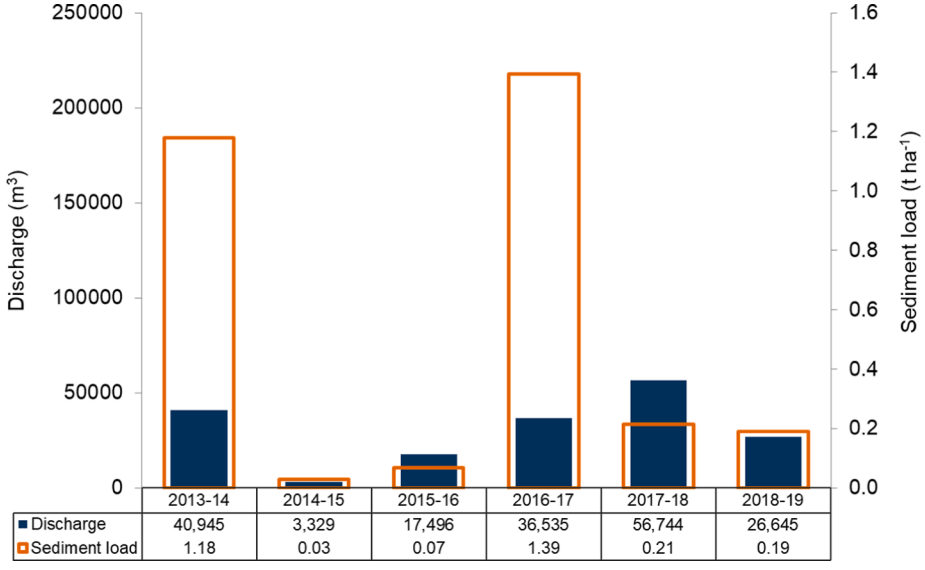

Fig. 3. Annual discharge (m^3) and suspended sediment load (t ha^{-1}) from 2013 to 2019.

Table 2
Correlation coefficients between selected rainfall event features (** − p < 0.05, * − p < 0.10, n = 111).

	Rainfall (mm)	Flood Q (m^3)	Q_max ($l\ s^{-1}$)	Max sediment concentration	Mean sediment concentration
I5 ($mm\ h^{-1}$)	**0.523	0.198	*0.326	*0.224	0.109
I60 ($mm\ h^{-1}$)	**0.751	*0.381	*0.495	0.186	0.140
D10 (mm)	−0.001	**0.488	*0.458	−0.037	−0.095
D20 (mm)	−0.089	**0.454	*0.418	−0.076	−0.151
D40 (mm)	−0.141	*0.370	*0.325	−0.185	−0.197
Q_max ($l\ s^{-1}$)	**0.526	**0.952		0.205	*0.306
Flood discharge (m^3)	**0.517		**0.952	0.096	0.191
Q base flow ($l\ s^{-1}$)	−0.224	**0.532	*0.497		0.179
Sediment load (t)	*0.374	**0.821	**0.859	**0.500	**0.619
Max. concentration	0.133	0.096	0.205		**0.763
Mean concentration	0.045	0.191	*0.306	**0.763	

4.2. Flood discharge and sediment production before and after implementing runoff and sediment control measure

Table 3 presents the median values for various rainfall, discharge and sediment variables according to the time of check dam construction. Median event rainfall in AFT was 13.0 mm and significantly higher than BEF with 9.0 (p < 0.05). Similarly, antecedent rainfall was also significantly higher in AFT than BEF, as well as D10 with 47.3 and 30.1 mm, respectively. Rainfall intensities were not significantly different, being median values slightly higher for AFT (Table 3). Flood discharge, maximum peak discharge and runoff coefficient of the events registered during AFT were significantly higher as compared to BEF. The median total event flood discharge was 104.9 m^3 BEF and 474.9 m^3 AFT and maximum peak discharge was significantly higher in AFT than BEF, with 87.2 and 22.5 $m^3 s^{-1}$, respectively. Hence, data indicate that flood discharge was not reduced as a consequence of the gully control measure installation. Suspended sediment load was not statistically different for events according to the time of gully control measure construction. On the contrary, the median of the mean suspended sediment concentrations was significantly higher in BEF than AFT with 0.31 $g\ l^{-1}$ and 0.11 g l^{-1}, respectively (p = 0.01). The gully control measures reduced the mean suspended sediment concentration by 65%. Although less pronounced, the medians of maximum sediment concentrations were also significantly different (BEF: 1.82 $g\ l^{-1}$, AFT: 0.98 $g\ l^{-1}$).

The first year after gully control measure construction 561 mm of rainfall were recorded, generating a total of 56,744 m^3 of flood discharge with a runoff coefficient of 10.2%. Taking into account the six years with information on suspended sediment load, this year was the highest value of discharge, being sediment production only ranked in position 3 (Fig. 3). The relationship between mean suspended sediment concentration and, flood discharge and runoff coefficient, grouped according to BEF and AFT, is presented in Fig. 4. The highest sediment concentration was observed in the rainfall events recorded before gully control measure implementation (Fig. 4a). Mean sediment concentration ranged from 0.08 to 0.2 g l^{-1} in rainfall events registered after implementing the control measures and that exceeded 10% runoff coefficient. Nevertheless, mean sediment concentration was >1.0 g l^{-1} in the events registered before implementing gully control measures (Fig. 4b). The relationship between event suspended sediment load and flood discharge, grouped according to BEF and AFT, is presented in Fig. 5a, showing significant correlations. Similarly, event suspended sediment and maximum peak discharge (Fig. 5b) are significantly correlated when grouped accordingly. The lower slope of the regression lines of the events registered during AFT, for both variables (flood discharge and maximum peak discharge), indicate the effect of check dams on reducing suspended sediment load.

4.3. Gully dynamics, sediment production and grain size of the sediments deposited in the channel

Sediment volume gain for the study period (2016–2019) was estimated to be 95.4 m^3, corresponding to a net deposition rate of 33.6 $m^3\ y^{-1}$. The net change before and after gully control measure construction was 42.7 m^3 and 52.7 m^3, respectively (Table 4). Considering an average bulk density of 1.5 $g\ cm^{-3}$ (Gómez-Gutiérrez, 2009) the annual change rate expressed in tons per year for BEF and AFT was 71.2 and 40.7.

Table 3
Median, lower and upper quartile of rainfall, discharge and suspended sediment variables for the events according to the time of check dam construction: Before (BEF) or after (AFT). Significant differences of the variables are indicated (** − p < 0.05, * − p < 0.10).

Variable	BEF	AFT	BEF	AFT	BEF	AFT	
	Median	Median	Lower	Lower	Upper	Upper	p-level
Rainfall (mm)	**8.98	**13.03	4.70	7.48	13.88	16.66	0.04
I5 ($mm\ h^{-1}$)	10.45	12.82	5.23	7.69	19.20	20.51	0.18
I10 ($mm\ h^{-1}$)	8.77	10.25	5.13	6.41	15.38	15.38	0.25
I30 ($mm\ h^{-1}$)	5.82	5.55	3.77	4.70	9.83	9.40	0.40
I60 ($mm\ h^{-1}$)	3.92	4.27	2.56	3.42	6.84	6.62	0.21
D24h (mm)	8.12	10.04	4.27	5.55	14.31	13.67	0.56
D5 (mm)	23.10	31.50	9.80	13.20	37.20	47.30	0.11
D10 (mm)	**30.10	**47.30	19.20	33.50	46.10	90.50	0.01
D20 (mm)	**53.00	**75.30	36.20	40.20	78.90	137.70	0.01
D40 (mm)	**101.00	**138.40	67.20	92.60	134.80	199.10	0.00
Q_max ($l\ s^{-1}$)	*22.54	*87.18	3.52	5.53	83.99	216.70	0.06
Discharge (m^3)	**190.34	**716.84	36.40	69.19	801.33	2,820.56	0.03
Flood discharge (m^3)	**104.98	**474.99	24.80	42.70	402.31	2,072.69	0.03
Q base flow ($l\ s^{-1}$)	**0.19	**1.05	0.03	0.22	1.14	4.72	0.01
Discharge base flow (m^3)	*34.96	*63.13	7.72	15.72	153.68	520.51	0.05
Runoff coefficient (%)	*1.32	*3.98	0.25	0.56	5.64	13.15	0.06
Sediment load (t)	0.07	0.32	0.01	0.01	0.48	0.75	0.64
Max. concentration ($g\ l^{-1}$)	*1.82	*0.98	0.83	0.56	4.17	3.05	0.07
Mean concentration ($g\ l^{-1}$)	**0.31	**0.11	0.12	0.08	1.26	0.42	0.01

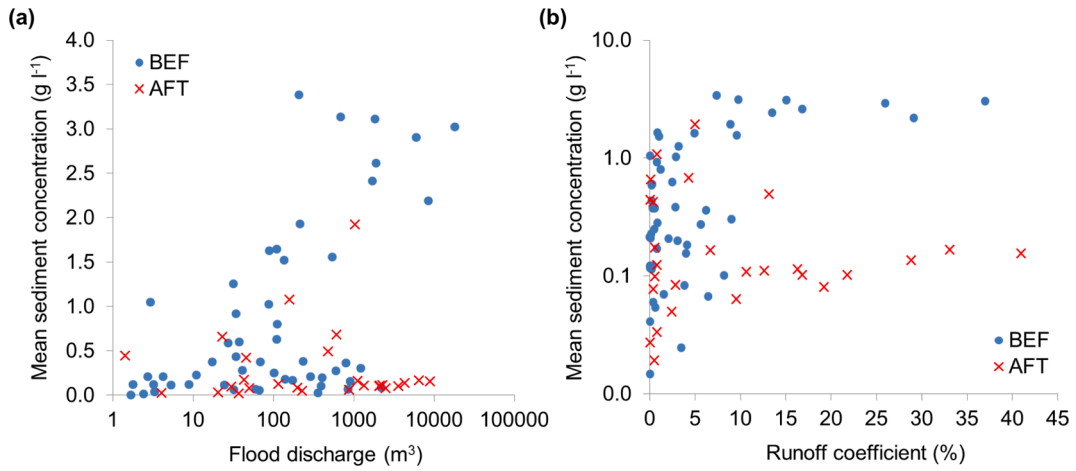

Fig. 4. Relationship between mean suspended sediment concentration and (a) total flood discharge and (b) runoff coefficients for events before and after implementing gully control measures.

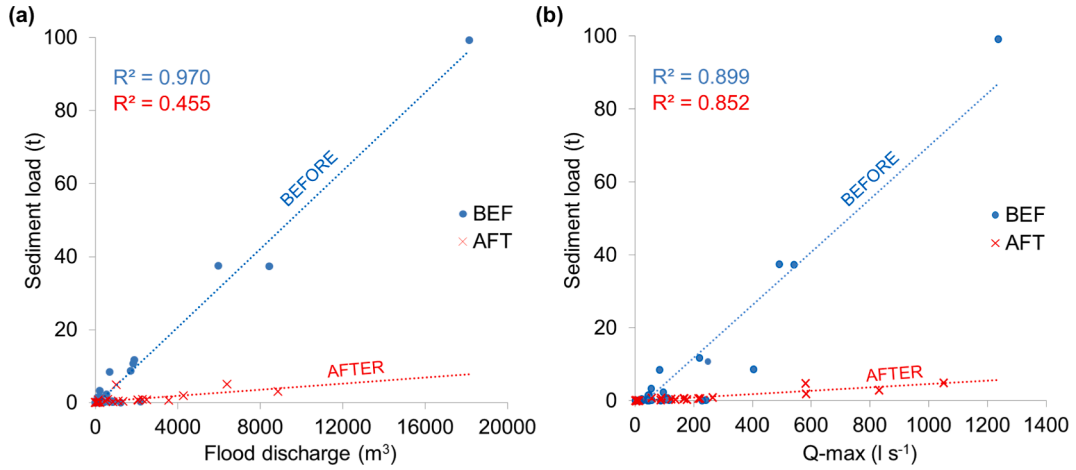

Fig. 5. Relationship between the event suspended sediment load and a) flood discharge and b) maximum peak discharge before and after implementing gully control measures ($p < 0.05$).

Table 4
Hydrological and sediment load data and topographic changes registered during the study period: erosion or deposition, net volume difference (NVD), maximum event rainfall (R_max), total flood discharge (Q), maximum peak discharge (Q_max), the number of times discharge exceeded 100 l s^{-1} (Q > 100 l s^{-1}), maximum rainfall intensity in 60 min (I60-max).

Period	Before	After
Duration	24/03/2016–10/02/2017	10/02/2017–25/01/2019
Erosion (m^3)	−8.0	−22.0
Deposition (m^3)	50.7	74.7
Net volumen difference (m^3)	42.7	52.7
NVD (t)	64.1	79.0
NVD rate (t y^{-1})	71.2	40.7
Rainfall amount (mm)	543.4	928.9
Events (N)	30	45
R_max (mm)	57.7	22.2
Q (m^3)	38334.1	40948.8
Q_max (l s^{-1})	1237.2	1052.3
Q > 100 l s^{-1} (N)	3	7
I60-max (mm h^{-1})	13.0	15.1
Runoff coefficient (%)	4.7	8.7
Sediment load (t)	137.0	23.8
Sediment yield (t km^{-2} y^{-1})	153.0	12.3

Suspended sediment load at the outlet of the catchment for the entire study period was 160.8 t, which represented a suspended sediment yield of 56.9 t km^{-2} y^{-1}. Before gully control measure construction, net deposition was lower than total sediment load at the outlet of the catchment. Contrary, after the implementation of the restoration measuresnet deposition was higher than sediment load. Comparing total sediment yield, BEF registered a much higher value than AFT, with 153 t km^{-2} y^{-1} and 12.3 t km^{-2} y^{-1}, respectively. It has to be taken into account that sediment load was lower in AFT despite registering potentially more erosive discharge events, as expressed by a greater number of peak floods > 100 l s^{-1} or a significantly higher median flood discharge (Table 3). Furthermore, as presented in the previous section, rainfall events with similar flood discharge produced different amounts of suspended sediment load.

Sediments trapped behind gully control measure had the highest content of coarse elements with 39%, compared with valley bottoms soils and other topographic positions. In addition, sediments deposited behind gully control measure was the location with the lowest content of fine fractions with 27 and 6% of silt and clay.

4.4. *Hydrological and sediment connectivity and gully geomorphic change*

The hydrological and sedimentological connectivity map shows the potential connection of water and sediment between the hillslope and

the valley-bottom gully. Fig. 6a presents the IC map calculated for the 2016 DTM of the catchment. The IC is higher along the slope of the main pediment, as well as the slope of the small pediment in the south-eastern part of the basin. The western part of the main pediment slope is poorly connected with the main channel due to the presence of a water pond. In contrast, the small pediment is highly connected to the main channel and the eastern part of the main pediment is also connected to the main channel with gentle slopes. The uppermost part of the catchment has low connectivity and corresponds to the upper part of the main pediment with low slope gradients. As expected, connectivity is generally highest close to the main channel and progressively decreases upslope (particularly at the right bank of the upper reach) although some parts with low connectivity close to the main channel can be highlighted. Across the right bank of the main channel, lines of high IC values are clearly aligned with cattle paths, which drive the flow and possibly capture a large proportion of sediment toward the gully (Fig. 6b). In addition, an unpaved road crosses the lower reach increasing connectivity towards the valley-bottom gully. This area shows scarce vegetation cover and patches of bare soil with evidences of soil erosion by water (erosion scars, tree root exposure), constituting potential source areas of sediments. In the upper reach, a new channel parallel to the main one developed influenced by a cattle path which caused the diversion of overland flow (Fig. 6c). In fact, the connectivity of the new channel was higher than that of the main channel before gully control measure construction. The left bank of the upper reach, particularly from GCD-01 to GCD-05, is an area strongly connected to the channel where eleven bank headcuts were formed. For instance, Fig. 6d displays the spatial relationship between the bank headcuts located between GCD-01 and GCD-03 and the flow pathways. Flow pathways with high values of connectivity are strongly connected to the gully, influencing the growth of bank headcuts.

A positive relationship between linear headcut retreat and the maximum IC value (calculated in the contributing area of each bank headcut) is indicated by a correlation coefficient of 0.821 ($p < 0.05$) (Fig. 7).

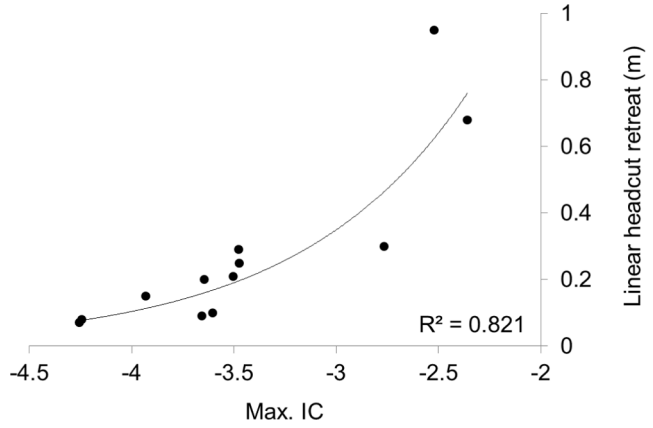

Fig. 7. Relationship between maximum IC values of contributing area and linear headcut retreat (mapped from SfM-derived orthophotographs for every survey).

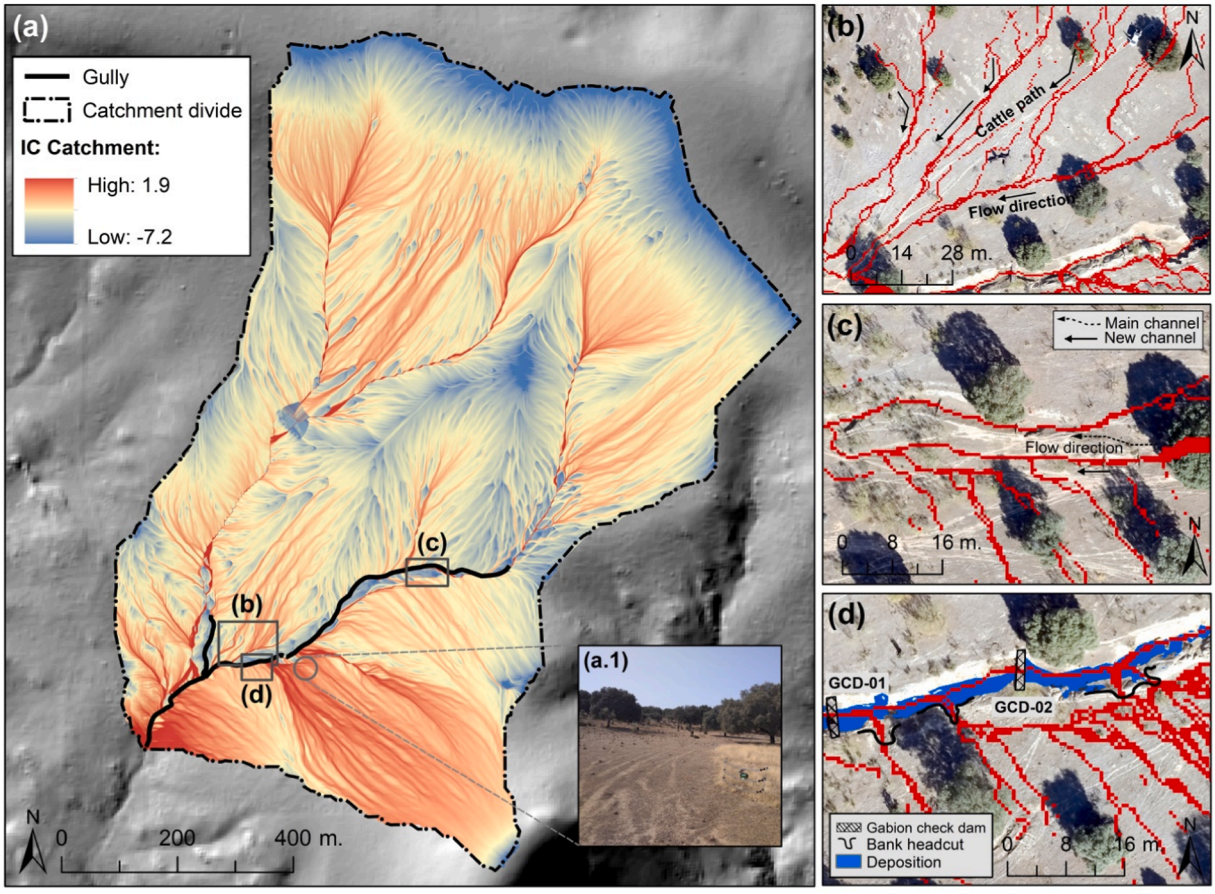

Fig. 6. (a) Connectivity index map calculated for the 2016 DTM of the Parapuños catchment and (a.1.) a photograph of the left bank hillslope, (b) cattle paths collecting and driving overland flow, (c) diversion of flow (coming from the left bank hillslope) from the main channel due to a depression originated by a cattle path and (d) detail of the left bank of the reach between GCD-01 and GCD-03 showing the spatial co-occurrence of bank headcuts and flow pathways draining the left hillslope. Red pixels in (b–d) are locations with contributing area > 100 m^2.

The setting up of gully control measures induced a change in channel topography leading to a decrease of structural connectivity. After the implementation of the control measures, an increase of connectivity was only observed downstream of five gully control measure (i.e., GCD-02, GCD-05, GCD-08, BCD-09 and BCD-13) and in the junction between the tributary and the upper reach. Before the implementation of the runoff and sediment control measures, connectivity increased in the headwater, in the new channel parallel to the main one (i.e., between F-16 and F-19, Fig. 8c) and in the left bank of a strongly degraded area where the wire fence was implemented later as a gully control measure. In addition, the values of connectivity experienced a decrease from 2017 between GW-01 and GW-04. Fig. 8 shows the spatial co-occurrence of connectivity with net volumes before and after gully control measure construction per strip. Lower values of connectivity (<1) highlight the areas where deposition dominated, which implied a decrease in connectivity due to reduced slope gradient and this decreases the ability to export sediments further down. For example, the section between F-07 and F-17 evolved from being a connected section to one with considerably reduced connectivity. Conversely, high values of connectivity were observed in the strips where erosion processes dominated.

The overlap of DoD and DoIC maps highlights the close relationship between deposition pattern and areas that experienced a decrease of IC. This tendency is supported by the cross-frequency analysis of DoD and DoIC values (Fig. 9d) calculated for the whole gully. Erosion prevailed slightly where IC increased, whereas deposition (78% of the total) was strongly associated with a decrease of IC. Fig. 9 presents some detailed examples overlapping DoDs and DoIC maps from 2016 to 2019 in the restored upper reach. For example, Fig. 9a shows how the values of connectivity decreased in the bank headcuts, particularly in those where livestock was excluded by a fence and BCDs were implemented. Connectivity not only decreased in the bank headcuts but also in large part of the isolated area. After gully control measure construction, the connectivity values decreased in the area upstream of the structures. This sharp decrease was due to the large sediment deposition experienced between GCD-01 and GCD-02 (Fig. 9c) and the sediments deposited behind GCD-06 (Fig. 9b). Nevertheless, a slight connectivity increase downstream GCD-02 and GCD-06 was observed. The values of connectivity also increased in two bank headcuts located between GCD-01 and GCD-03 (Fig. 9c).

5. Discussion

5.1. The role of gully control measures on runoff production and sediment yield

Check dams did not affect discharge, but did reduce sediment concentration and sediment load. Similar flood discharges resulted in different sediment load with a lower suspended sediment concentration after gully control measure construction. Previous work has also found that GCDs capture, mainly coarse sediments (Hassanli et al., 2009; Nichols et al., 2016). In our study, sediments trapped behind GCDs have the lowest contents of clay, silt and sand, as compared to the channel banks, which indicates impoverishment of fine fractions, which presumably corresponds to sediment leaving the catchment as suspended load. Additionally, in Parapuños check dams also reduced the fine fraction of sediments compared to other studies where silt and clay were not reduced by GCDs (Koci et al., 2021) or only in reaches of the gully with very low slope gradients (Abedini et al., 2012; Hassanli et al., 2009). Our findings agree with the results of studies that analyzed the impact of porous check dams on sediment load (Borja et al., 2018; Polyakov et al., 2014). For example, a remarkable effectiveness of check dams on reducing sediment yield was found by Mishra et al. (2007), Boix-Fayos et al. (2007) and Borja et al. (2018) who observed that porous and small check dams reduced the sediment yield by 64–85%. This reduction in sediment concentration may be favoured by the combination of different runoff and sediment control measures implemented in a catchment, for instance Koci et al. (2021) showed a reduction of gully total sediment yield by >80% with the

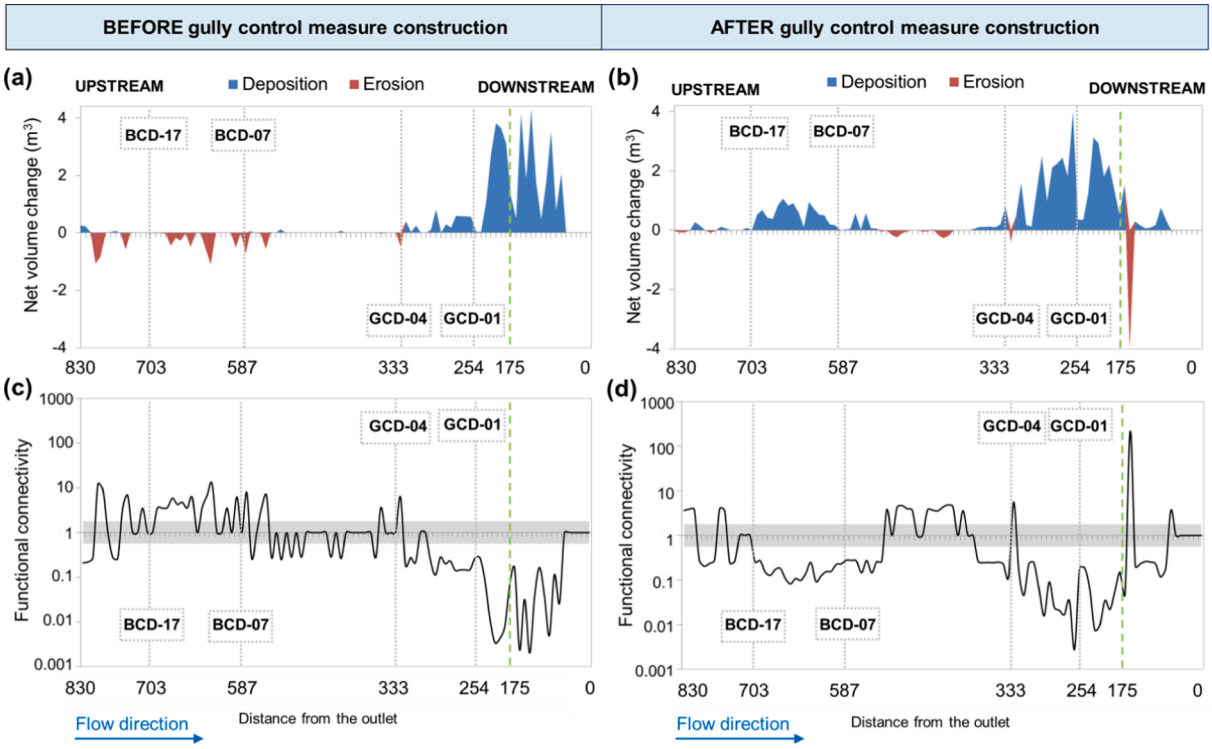

Fig. 8. Net volume change (a) before and (b) after gully control measure construction, (c) functional connectivity (Cv-strip) along the main channel before gully control measure construction and (d) after gully control measure construction. Dotted grey lines indicate the location of GCD-01, GCD-04, BCD-07 and BCD-17 and the dotted green line displays the beginning of the lower reach.

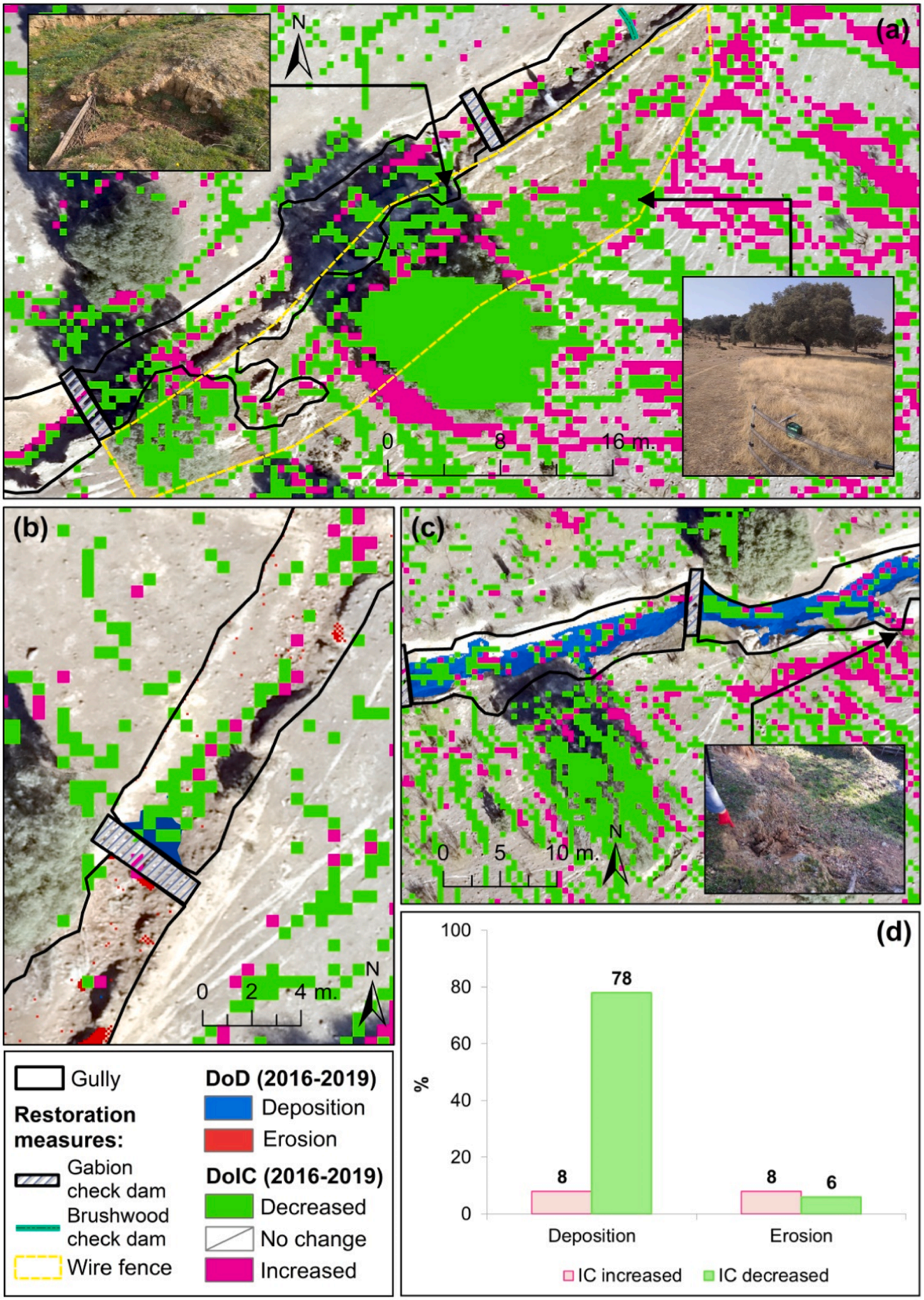

Fig. 9. Difference of connectivity index (DoIC) maps and superposed DoD from 2016 and 2019 at three different locations: (a) detail of the upper reach with bank headcuts that were fenced to exclude livestock, (b) GCD-06, (c) GCD-01 and GCD-02 area and (d) IC increase and decrease for the whole channel of areas with either cross-frequency of erosion or deposition (DoD 2017–2019; i.e., geomorphic changes after gully control measures).

implementation of GCDs and cattle exclusion and Heede (1978) reduced the catchment sediment yield by >90% with the combination of GCDs, grassed waterway and reduction in livestock grazing pressure.

Concrete check dams were also effective in reducing sediment yield (Xu et al., 2013; Vaezi et al., 2017; Li et al., 2017). For example, Ran et al. (2008) analyzed a dataset of available figures previously published, concluding that in the watershed of the Kuye River, the establishment of check dams caused a decrease in sediment load of 37% in a period of 26 years. Zhang et al. (2021) found in the same watershed that check dams reduced suspended sediment concentration by 54% in 2006 and 31% in 2016. A similar trend was observed by Fortugno et al. (2017) in a watershed in Italy where check dams reduced the sediment yield by 30–35%.

Regarding the gully dynamics and sediment production, net deposition registered in the channel was lower than total sediment load measured at the outlet of the catchment before gully control measure construction. The gully, therefore, facilitated a rapid transport of water and sediments downstream. According to Poesen et al. (2003) and Capra et al. (2005), gullies perform as effective links between the upper and lower lands of a basin, increasing flow sediment transport capacity and sediment connectivity. Contrary, after runoff and sediment control measure construction net deposition in the channel was higher in 55.2 t than the sediment load at the outlet (23.8 t), hence the effect of check dams on retaining sediments was roughly 50%. The sediment load at the outlet was lower after gully control measure construction despite more potentially erosive discharge events were registered in this period, as expressed by a greater number of peak floods > 100 l s^{-1} or catchment runoff coefficients. A total of 3 and 7 rainfall events with a peak floods > 100 l s^{-1} was registered before and after runoff and sediment control measure construction, respectively.

In similar environments, gully erosion represents the dominant source of sediments registered at the outlet of the catchments (Koci et al., 2017; Waterhouse et al., 2017; Wilkinson et al., 2018). In our study site, the predominance of net deposition in the gully and the high amount of sediment exported at the outlet before gully control measure construction suggest and important sediment production by sheet wash at hillslopes. The erosion rates registered by Schnabel et al. (2010) were similar to those presented in this study (2.25 t ha^{-1} y^{-1}) for periods when hillslopes had a reduced degree of vegetation cover (<50%) with soil loss of 1.34 t ha^{-1} y^{-1}, due, in part, to high stocking density. Kosmas et al. (2015) highlighted the relation between livestock density and soil erosion rates in a region with overgrazing in southern Europe (Crete Island, Greece) and Gutiérrez et al. (2009) found a relationship between gully erosion and livestock density.

The sediment yield at Parapuños catchment before gully control measure construction was similar to the sediment yield in other Mediterranean catchments (Vanmaercke et al., 2011). According to Vanmaercke et al.'s work, in the Mediterranean >50% of catchments have sediment yields higher than 2 t ha^{-1} y^{-1}. Nevertheless, the temperate and relatively gentle slope catchments of Western, Northern and Central Europe generally have relatively low sediment yield (with approximately 50% of the catchments lower than 0.4 t ha^{-1} y^{-1}). Vanmaercke et al. (2011) demonstrated the high variability of sediment yield in Europe, also for Mediterranean catchments with sizes similar to our study area. Climatic dynamics are highly variable in the Mediterranean because of several atmospheric and geographical factors. Rainfall seasonality determines sediment transport as rainfall regimes control primarily runoff production and soil erosion by water (García-Ruiz et al., 2013). It is typical in the Mediterranean region that few rainfall events may contribute to most of the soil eroded by water (González-Hidalgo et al., 2007).

5.2. *The effect of gully control measures and grazing on sediment connectivity*

The connectivity analysis, carried out using IC, highlighted how cattle livestock grazing determines preferential sediment pathways in the studied area. Cattle livestock paths drive sediment fluxes toward the gully suggesting that this activity plays an important role in increasing sediment connectivity at the catchment scale. Grazing and trampling by sheep and cattle reduces vegetation cover and enhances runoff and erosion in dehesa catchments (Gómez-Gutiérrez et al., 2012; Gutiérrez et al., 2009; Schnabel, 1997). Unpaved roads and cattle paths increased the routing of water in the catchment, limiting water infiltration and concentrating flows. Previous research has highlighted the critical role that unpaved roads and trails play in generating runoff on woodland-grassland ecosystem (Croke et al., 2005; Gómez-Gutiérrez et al., 2018; Sidle et al., 2004). Commonly, trails and roads display low hydraulic conductivity (Koci et al., 2020), which capture overland flow from adjacent areas and hillslopes, driving the water effectively to the channel or gully (Sidle and Ziegler, 2010; Sidle et al., 2006). Livestock tracks not only contribute to divert runoff along well-defined pathways, they also increase channel-hillslope connectivity. According to van der Waal and Rowntree (2018), cattle paths can notably increase drainage density. In this example, in a small catchment situated in the Southeast of South Africa the drainage density was increased by 159%. In Parapuños, flow pathways with high values of connectivity in the catchment were strongly connected to the gully that influenced the growth of channel headcuts and bank headcuts (Gutiérrez et al., 2009; Gomez-Gutierrez et al., 2018). For instance, the bank headcuts located upstream GCD-02 and displayed in the Fig. 6d is likely to split in two different directions follow the flow pathway.

The effect of human activities on sediment connectivity is recently gaining particular attention in the literature (Llena et al., 2019; López-Vicente et al., 2020; Persichillo et al., 2018). A recent work by López-Vicente et al. (2020) investigated changes in sediment connectivity due to forest fires in three Mediterranean headwater catchments analyzing also the role of post-fire practices such as salvage logging, skid trails and check dams. To this end, the authors tested two different computation targets: the stream network and the outlet. In our study we focused just on the catchment outlet to characterize in terms of connectivity the main stream and to compare it with DoD results along the channel. However, López-Vicente et al. (2020) argue that the connectivity assessment in regards to the stream network may be more suitable to predict sediment transport induced by low-frequency intense rainfall events. Future work in our catchment, more focused on hillslope-to-channel connectivity, may certainly consider this target scenario.

In another Mediterranean catchment, Calsamiglia et al. (2018) found that check dam terraces, built to control overland flow and prevent erosion, reduced the highest IC values mainly concentrated along preferential pathways where erosional processes are most likely to occur. In the same work, the barriers also showed relevant decoupling effects along the thalwegs. In fact, the widespread implementation of this type of control measures, on the one hand, is mainly intended to locally retain sediment and reduce erosion along channels (Alfonso-Torreño et al., 2021), on the other hand, these runoff and sediment control measures considerably reduced values of IC in the channel (i.e., longitudinal connectivity). Similar effects were found by Fryirs (2013) and Marchi et al. (2019), who observed that this kind of measures disconnect the hydrological and sedimentological dynamics in the channel. Nevertheless, other studies (e.g., Cucchiaro et al., 2019; Heckmann et al., 2018; Poeppl et al., 2017; Wohl et al., 2017) highlighted the effect of check dams on reducing lateral (i.e., hillslope-to-channel) connectivity.

In this work an integrated approach encompassing multi-temporal analyses of topographic changes (DoD) and sediment connectivity (DoIC) has been applied in order to fully address the issue related to the impact of check dams on sediment dynamics in the study catchment. This kind of approach has been already applied in other contexts and geographical areas (e.g., Cucchiaro et al., 2019; Martini et al., 2019) to analyze natural and anthropic disturbances and the findings of our study seems to confirm its validity stressing the need of such a tool for better sediment management and control planning. In particular, we found a

notable correspondence between DoD and DoIC patterns. This outcome suggests that DoIC could be used as a predictive variable of future sediment transfer processes: areas featuring an increase of sediment connectivity through time should be carefully monitored because they are potential areas that may feature erosion in the short-term. In general, after the implementation of the runoff and sediment control measures we observed that structural connectivity decreased in the upper reach and increased only downstream of two GCDs and in bank headcuts without the influence of the exclusion measure. The wire fence not only helped to reduce erosion in bank headcuts (Alfonso-Torreño et al., 2021), but also reduced the values of IC in bank headcuts within the isolated area from sheep and cattle. According to Kirkby and Bracken (2009) and (Wilkinson et al., 2018), the implementation of livestock exclusion (by fencing) measures in the intersection points between hydrological flow pathways and the channel favors the revegetation and the reduction of overland flow concentration in the specific contributing area. In other places, revegetation of hillslopes reduced the erosive effect of runoff, controlling gullying and sediment yields (e.g., Chen and Cai, 2006; Talema et al., 2019). Runoff and sediment control measures implemented perpendicular to the gully (i.e., GCDs and BCDs), combined with livestock exclusion through fencing adjacent to the channel or in hillslopes, facilitated the reduction in sediment transport as also observed Bartley et al. (2020).

6. Conclusions

The implementation of check dams in the channel reduced the suspended sediment concentrations at the outlet by 65% but no effect was detected on flood discharge. The mean sediment concentration was positively correlated with maximum peak flow but no relationship was detected with the rainfall variables. The effect of runoff and sediment control measures on changes in the gully dynamics and sediment production was also remarkable. The combination of rainfall, discharge and suspended sediment data at the event scale with multi-temporal topographic surveys using an UAV and SfM photogrammetry allowed the comparison of gully dynamics with sediment production at the outlet of the catchment. Net deposition in the channel was lower than total sediment load at the outlet of the catchment before gully control measure construction. Contrary, after gully control measure construction net deposition in the channel was higher than sediment load at the outlet.

The hydrological and sedimentological connectivity map showed the potential link of water and sediment between the hillslope and the channel. As it was expected, connectivity was generally higher close to the main channel. Flow pathways with high values of connectivity are strongly connected to the gully, influencing the growth of bank headcuts and the deposition behind check dams. In addition, lines of high IC values are clearly aligned with cattle paths. The effect of gully control measures (i.e., GCDs, BCDs and livestock exclusion through fencing) on longitudinal connectivity was remarkable. The values of connectivity decreased in the upper reach after the implementation of the runoff and sediment control measures. This decrease took place in areas where deposition dominated and also in the bank headcuts restored by BCDs and excluded from livestock by fencing. The isolated area from livestock favored revegetation, and in consequence of this, promoted a decrease of sediment connectivity and a potential reduction of sediment supply to the channel. Conversely, the IC increased in the strips where erosion processes dominated, e.g., downstream of two GCDs and in bank headcuts without the influence of the exclusion measure. These critical areas should be the target to prevent gully erosion through the effective implementation of soil engineering and bioengineering structural measures. This study demonstrated that the connectivity framework is an effective tool for assessing the changes on longitudinal and lateral connectivity produced by the implementation of runoff and sediment control measures.

Declaration of Competing Interest

The authors declare that they have no known competing financial interests or personal relationships that could have appeared to influence the work reported in this paper.

Acknowledgments

The present study was financed by the Spanish Ministry of Economy and Competitiveness (file number CGL2014-54822-R) and Alberto Alfonso-Torreño was the beneficiary of a PhD fellowship from the regional government, i.e. Junta de Extremadura (PD16004).

Appendix A. Supplementary material

Supplementary data to this article can be found online at https://doi.org/10.1016/j.catena.2022.106259.

References

Abedini, M., Said, M.A.M., Ahmad, F., 2012. Effectiveness of check dam to control soil erosion in a tropical catchment (The Ulu Kinta Basin). Catena 97, 63–70. https://doi.org/10.1016/j.catena.2012.05.003.

Alfonso-Torreño, A., Gómez-Gutiérrez, Á., Schnabel, S., 2021. Dynamics of erosion and deposition in a partially restored valley-bottom gully. Land 10, 62. https://doi.org/10.3390/land10010062.

Alfonso-Torreño, A., Gómez-Gutiérrez, Á., Schnabel, S., Lavado Contador, J.F., de Sanjosé Blasco, J.J., Sánchez, F.M., 2019. sUAS, SfM-MVS photogrammetry and a topographic algorithm method to quantify the volume of sediments retained in check-dams. Sci. Total Environ. 678, 369–382. https://doi.org/10.1016/j.scitotenv.2019.04.332.

Bakker, M.M., Govers, G., Rounsevell, M.D.A., 2004. The crop productivity–erosion relationship: an analysis based on experimental work. Catena 57 (1), 55–76. https://doi.org/10.1016/j.catena.2003.07.002.

Bartley, R., Poesen, J., Wilkinson, S., Vanmaercke, M., 2020. A review of the magnitude and response times for sediment yield reductions following the rehabilitation of gullied landscapes. Earth Surf. Proc. Land. 45 (13), 3250–3279. https://doi.org/10.1002/esp.4963.

Belmonte, F., Romero Díaz, A., Martínez Lloris, M., 2005. Erosión en cauces afectados por obras de corrección hidrológica (Cuenca del Río Quípar, Murcia). Papeles de Geografía 71–83.

Boardman, J., Poesen, J., Evans, R., 2003. Socio-economic factors in soil erosion and conservation. Environ. Sci. Policy 6 (1), 1–6. https://doi.org/10.1016/S1462-9011(02)00120-X.

Boix-Fayos, C., Barberá, G.G., López-Bermúdez, F., Castillo, V.M., 2007. Effects of check dams, reforestation and land-use changes on river channel morphology: Case study of the Rogativa catchment (Murcia, Spain). Geomorphology 91 (1-2), 103–123. https://doi.org/10.1016/j.geomorph.2007.02.003.

Borja, P., Molina, A., Govers, G., Vanacker, V., 2018. Check dams and afforestation reducing sediment mobilization in active gully systems in the Andean mountains. Catena 165, 42–53. https://doi.org/10.1016/j.catena.2018.01.013.

Borselli, L., Cassi, P., Torri, D., 2008. Prolegomena to sediment and flow connectivity in the landscape: a GIS and field numerical assessment. Catena 75 (3), 268–277. https://doi.org/10.1016/j.catena.2008.07.006.

Bracken, L.J., Croke, J., 2007. The concept of hydrological connectivity and its contribution to understanding runoff-dominated geomorphic systems. Hydrol. Processes: Int. J. 21 (13), 1749–1763. https://doi.org/10.1002/hyp.6313.

Bracken, L.J., Turnbull, L., Wainwright, J., Bogaart, P., 2015. Sediment connectivity: a framework for understanding sediment transfer at multiple scales. Earth Surf. Proc. Land. 40 (2), 177–188. https://doi.org/10.1002/esp.3635.

Brierley, G., Fryirs, K., Jain, V., 2006. Landscape connectivity: the geographic basis of geomorphic applications. Area 38 (2), 165–174. https://doi.org/10.1111/j.1475-4762.2006.00671.x.

Calle, M., Calle, J., Alho, P., Benito, G., 2020. Inferring sediment transfers and functional connectivity of rivers from repeat topographic surveys. Earth Surf. Proc. Land. 45 (3), 681–693. https://doi.org/10.1002/esp.4765.

Calsamiglia, A., Fortesa, J., García-Comendador, J., Lucas-Borja, M.E., Calvo-Cases, A., Estrany, J., 2018. Spatial patterns of sediment connectivity in terraced lands: Anthropogenic controls of catchment sensitivity. Land Degrad. Dev. 29 (4), 1198–1210. https://doi.org/10.1002/ldr.2840.

Capra, A., Mazzara, L.M., Scicolone, B., 2005. Application of the EGEM model to predict ephemeral gully erosion in Sicily, Italy. Catena 59 (2), 133–146. https://doi.org/10.1016/j.catena.2004.07.001.

Castillo, V.M., Mosch, W.M., García, C.C., Barberá, G.G., Cano, J.A.N., López-Bermúdez, F., 2007. Effectiveness and geomorphological impacts of check dams for soil erosion control in a semiarid Mediterranean catchment: El Cárcavo (Murcia, Spain). Catena 70 (3), 416–427. https://doi.org/10.1016/j.catena.2006.11.009.

Cavalli, M., Goldin, B., Comiti, F., Brardinoni, F., Marchi, L., 2017. Assessment of erosion and deposition in steep mountain basins by differencing sequential digital terrain

models. Geomorphology 291, 4–16. https://doi.org/10.1016/j.geomorph.2016.04.009.
Cavalli, M., Trevisani, S., Comiti, F., Marchi, L., 2013. Geomorphometric assessment of spatial sediment connectivity in small Alpine catchments. Geomorphology 188, 31–41. https://doi.org/10.1016/j.geomorph.2012.05.007.
Cavalli, M., Vericat, D., Pereira, P., 2019. Mapping water and sediment connectivity. Sci. Total Environ. 673, 763–767. https://doi.org/10.1016/j.scitotenv.2019.04.071.
Cavalli, M., Crema, S., Marchi, L., 2020. Structural sediment connectivity assessment through a geomorphometric approach: review of recent applications. In Massimiliano Alvioli, Ivan Marchesini, Laura Melelli & Peter Guth, eds. Proceedings of the Geomorphometry 2020 Conference_57, 212-215, https://doi.org/10.30437/GEOMORPHOMETRY2020_5.
Ceballos, A., Schnabel, S., 1998. Hydrological behaviour of a small catchment in the dehesa landuse system (Extremadura, SW Spain). J. Hydrol. 210 (1-4), 146–160. https://doi.org/10.1016/S0022-1694(98)00180-2.
Cerdà, A., Schnabel, S., Ceballos, A., Gómez-Amelia, D., 1998. Soil hydrological response under simulated rainfall in the Dehesa land system (Extremadura, SW Spain) under drought conditions. Earth Surf. Proc. Land. 23 (3), 195–209. https://doi.org/10.1002/(SICI)1096-9837(199803)23:3<195::AID-ESP830>3.0.CO;2-I.
Conesa García, C., 2004. Los diques de retención en cuencas de régimen torrencial: diseño, tipos y funciones. Nimbus: Revista de climatología, meteorología y paisaje 13–15, 125–142.
Crema, S., Cavalli, M., 2018. SedInConnect: a stand-alone, free and open source tool for the assessment of sediment connectivity. Comput. Geosci. 111, 39–45. https://doi.org/10.1016/j.cageo.2017.10.009.
Croke, J., Mockler, S., Fogarty, P., Takken, I., 2005. Sediment concentration changes in runoff pathways from a forest road network and the resultant spatial pattern of catchment connectivity. Geomorphology 68 (3-4), 257–268. https://doi.org/10.1016/j.geomorph.2004.11.020.
Cucchiaro, S., Cavalli, M., Verica, D., Crema, S., Llena, M., Beinat, A., Marchi, L., Cazorzi, F., 2019. Geomorphic effectiveness of check dams in a debris-flow catchment using multi-temporal topographic surveys. Catena 174, 73–83. https://doi.org/10.1016/j.catena.2018.11.004.
Chen, H., Cai, Q., 2006. Impact of hillslope vegetation restoration on gully erosion induced sediment yield. Science in China Series D 49 (2), 176–192. https://doi.org/10.1007/s11430-005-0177-4.
Chow, V., Maidment, D., Mays, L., 1988. Applyed Hydrology. New York.
Eichhorn, M.P., Paris, P., Herzog, F., Incoll, L.D., Liagre, F., Mantzanas, K., Mayus, M., Moreno, G., Papanastasis, V.P., Pilbeam, D.J., Pisanelli, A., Dupraz, C., 2006. Silvoarable systems in Europe–past, present and future prospects. Agrofor. Syst. 67 (1), 29–50. https://doi.org/10.1007/s10457-005-1111-7.
Fortugno, D., Boix-Fayos, C., Bombino, G., Denisi, P., Quiñonero Rubio, J.M., Tamburino, V., Zema, D.A., 2017. Adjustments in channel morphology due to land-use changes and check dam installation in mountain torrents of Calabria (southern Italy). Earth Surf. Proc. Land. 42 (14), 2469–2483. https://doi.org/10.1002/esp.4197.
Frankl, A., Nyssen, J., Vanmaercke, M., Poesen, J., 2021. Gully prevention and control: techniques, failures and effectiveness. Earth Surf. Proc. Land. 46 (1), 220–238. https://doi.org/10.1002/esp.5033.
Fryirs, K., 2013. (Dis) Connectivity in catchment sediment cascades: a fresh look at the sediment delivery problem. Earth Surf. Proc. Land. 38 (1), 30–46. https://doi.org/10.1002/esp.3242.
García-Ruiz, J.M., Nadal-Romero, E., Lana-Renault, N., Beguería, S., 2013. Erosion in Mediterranean landscapes: Changes and future challenges. Geomorphology 198, 20–36.
Gifford, G.F., Thomas, D.B., Coltharp, G.B., Coltharp, B., 1977. Effects of gully plugs and contour furrows on erosion and sedimentation in Cisco Basin. Utah 30 (4), 290. https://doi.org/10.2307/3897308.
González-Romero, J., López-Vicente, M., Gómez-Sánchez, E., Peña-Molina, E., Galletero, P., Plaza-Alvarez, P., Moya, D., De las Heras, J., Lucas-Borja, M.E., 2021. Post-fire management effects on sediment (dis) connectivity in Mediterranean forest ecosystems: Channel and catchment response. Earth Surf. Proc. Land. 46 (13), 2710–2727. https://doi.org/10.1002/esp.5202.
Gómez-Gutiérrez, Á., Schnabel, S., De Sanjosé, J.J., Contador, F.L., 2012. Exploring the relationships between gully erosion and hydrology in rangelands of SW Spain. Zeitschrift für Geomorphologie, Supplementary Issues 56 (1), 27–44. https://doi.org/10.1127/0372-8854/2012/S-00071.
Gutiérrez, Á.G., Schnabel, S., Contador, F.L., 2009. Gully erosion, land use and topographical thresholds during the last 60 years in a small rangeland catchment in SW Spain. Land Degrad. Dev. 20 (5), 535–550. https://doi.org/10.1002/ldr.931.
Gomez-Gutierrez, A., Schnabel, S., Lavado-Contador, J.F., Sanjosé Blasco, J.J., Atkinson Gordo, A.D.J., Pulido-Fernández, M., Sánchez-Fernández, M., 2018. Studying the influence of livestock pressure on gully erosion in rangelands of SW Spain by means of the UAV SfM workflow. Boletín de la Asociación de Geógrafos Españoles 78, 66–68. https://doi.org/10.21138/bage.2712.
González-Hidalgo, J.C., Peña-Monné, J.L., de Luis, M., 2007. A review of daily soil erosion in Western Mediterranean areas. Catena 71 (2), 193–199. https://doi.org/10.1016/j.catena.2007.03.005.
Hassanli, A.M., Nameghi, A.E., Beecham, S., 2009. Evaluation of the effect of porous check dam location on fine sediment retention (a case study). Environ. Monit. Assess. 152 (1-4), 319–326. https://doi.org/10.1007/s10661-008-0318-2.
Heckmann, T., Cavalli, M., Cerdan, O., Foerster, S., Javaux, M., Lode, E., Smetanová, A., Vericat, D., Brardinoni, F., 2018. Indices of sediment connectivity: opportunities, challenges and limitations. Earth Sci. Rev. 187, 77–108. https://doi.org/10.1016/j.earscirev.2018.08.004.
Heckmann, T., Vericat, D., 2018. Computing spatially distributed sediment delivery ratios: inferring functional sediment connectivity from repeat high-resolution digital elevation models. Earth Surf. Proc. Land. 43 (7), 1547–1554. https://doi.org/10.1002/esp.4334.
Heede, B.H., 1978. Designing gully control systems for eroding watersheds. Environ. Manage. 2 (6), 509–522.
Herguido Sevillano, E., Lavado Contador, J.F., Pulido, M., Schnabel, S., 2017. Spatial patterns of lost and remaining trees in the Iberian wooded rangelands. Appl. Geogr. 87, 170–183. https://doi.org/10.1016/j.apgeog.2017.08.011.
Hooke, J., 2003. Coarse sediment connectivity in river channel systems: a conceptual framework and methodology. Geomorphology 56 (1-2), 79–94. https://doi.org/10.1016/S0169-555X(03)00047-3.
Horton, R.E., 1933. The role of infiltration in the hydrological cycle. Trans. Am. Geophys. Union 14, 446–460.
Kirkby, M.J., Bracken, L.J., 2009. Gully processes and gully dynamics. Earth Surface Processes Landforms: J. Brit. Geomorphol. Res. Group 34 (14), 1841–1851. https://doi.org/10.1002/esp.1866.
Kizos, T., Plieninger, T., 2008. Agroforestry systems change in the Mediterranean: some evidence from Greek and Spanish examples. In: In Proceedings of International conference“ studying, modeling and sense making of planet Earth”, pp. 1–6.
Koci, J., Jarihani, B., Leon, J.X., Sidle, R.C., Wilkinson, S.N., Bartley, R., 2017. Assessment of UAV and ground-based structure from motion with multi-view stereo photogrammetry in a gullied savanna catchment. ISPRS Int. J. Geo-Inf. 6, 328. https://doi.org/10.3390/ijgi6110328.
Koci, J., Sidle, R.C., Jarihani, B., Cashman, M.J., 2020. Linking hydrological connectivity to gully erosion in savanna rangelands tributary to the Great Barrier Reef using structure-from-motion photogrammetry. Land Degrad. Dev. 31 (1), 20–36. https://doi.org/10.1002/ldr.3421.
Koci, J., Wilkinson, S.N., Hawdon, A.A., Kinsey-Henderson, A.E., Bartley, R., Goodwin, N.R., 2021. Rehabilitation effects on gully sediment yields and vegetation in a savanna rangeland. Earth Surf. Proc. Land. 46 (5), 1007–1025. https://doi.org/10.1002/esp.5076.
Kosmas, C., Detsis, V., Karamesouti, M., Kounalaki, K., Vassiliou, P., Salvati, L., 2015. Exploring long-term impact of grazing management on land degradation in the socio-ecological system of Asteroussia Mountains, Greece. Land 4, 541–559. https://doi.org/10.3390/land4030541.
Lana-Renault, N., Latron, J., Regüés, D., Serrano, P., Nadal, E., 2008. Diferencias estacionales en la generación de escorrentía en una pequeña cuenca de campos abandonados en el Pirineo Central. Cuadernos de investigación geográfica 34 (0), 23. https://doi.org/10.18172/cig.vol34iss010.18172/cig.1205.
Lehotský, M., Rusnák, M., Kidová, A., Dudžák, J., 2018. Multitemporal assessment of coarse sediment connectivity along a braided-wandering river. Land Degrad. Dev. 29 (4), 1249–1261. https://doi.org/10.1002/ldr.2870.
Li, E., Mu, X., Zhao, G., Gao, P., Sun, W., 2017. Effects of check dams on runoff and sediment load in a semi-arid river basin of the Yellow River. Stoch. Env. Res. Risk Assess. 31 (7), 1791–1803. https://doi.org/10.1007/s00477-016-1333-4.
López-Vicente, M., Poesen, J., Navas, A., Gaspar, L., 2013. Predicting runoff and sediment connectivity and soil erosion by water for different land use scenarios in the Spanish Pre-Pyrenees. Catena 102, 62–73. https://doi.org/10.1016/j.catena.2011.01.001.
López-Vicente, M., Nadal-Romero, E., Cammeraat, E.L.H., 2017. Hydrological connectivity does change over 70 years of abandonment and afforestation in the Spanish Pyrenees. Land Degrad. Dev. 28, 1298–1310. https://doi.org/10.1002/ldr.2531.
López-Vicente, M., González-Romero, J., Lucas-Borja, M.E., 2020. Forest fire effects on sediment connectivity in headwater sub-catchments: Evaluation of indices performance. Sci. Total Environ. 732, 139206. https://doi.org/10.1016/j.scitotenv.2020.139206.
Llena, M., Vericat, D., Cavalli, M., Crema, S., Smith, M., 2019. The effects of land use and topographic changes on sediment connectivity in mountain catchments. Sci. Total Environ. 660, 899–912. https://doi.org/10.1016/j.scitotenv.2018.12.479.
Marchi, L., Comiti, F., Crema, S., Cavalli, M., 2019. Channel control works and sediment connectivity in the European Alps. Sci. Total Environ. 668, 389–399. https://doi.org/10.1016/j.scitotenv.2019.02.416.
Martín-Rosales, W., Cerón, J., López-Chicano, M., Fernández, I., 2003. Aspectos ambientales e hidrogeológicos de la Gruta de las Maravillas (Huelva, España). Boletín geológico y minero 114, 247–254.
Martini, L., Picco, L., Iroumé, A., Cavalli, M., 2019. Sediment connectivity changes in an Andean catchment affected by volcanic eruption. Sci. Total Environ. 692, 1209–1222. https://doi.org/10.1016/j.scitotenv.2019.07.303.
Mishra, A., Froebrich, J., Gassman, P.W., 2007. Evaluation of the SWAT model for assessing sediment control structures in a small watershed in India. Trans. ASABE 50, 469–477. https://doi.org/10.13031/2013.22637.
Nichols, M.H., Polyakov, V.O., Nearing, M.A., Hernandez, M., 2016. Semiarid watershed response to low-tech porous rock check dams. Soil Sci. 181, 275–282. https://doi.org/10.1097/SS.0000000000000160.
Pathak, P., Wani, S.P., Sudi, R., 2005. Gully control in SAT watersheds. International Crops Research Institute for the Semi-arid Tropics.
Persichillo, M.G., Bordoni, M., Cavalli, M., Crema, S., Meisina, C., 2018. The role of human activities on sediment connectivity of shallow landslides. Catena 160, 261–274. https://doi.org/10.1016/j.catena.2017.09.02.
Pinto-Correia, T., Ribeiro, N., Sá-Sousa, P., 2011. Introducing the montado, the cork and holm oak agroforestry system of Southern Portugal. Agrofor. Syst. 82 (2), 99–104. https://doi.org/10.1007/s10457-011-9388-1.

Poeppl, R.E., Keesstra, S.D., Maroulis, J., 2017. A conceptual connectivity framework for understanding geomorphic change in human-impacted fluvial systems. Geomorphology 277, 237–250. https://doi.org/10.1016/j.geomorph.2016.07.033.
Poesen, J., Nachtergaele, J., Verstraeten, G., Valentin, C., 2003. Gully erosion and environmental change: importance and research needs. Catena 50 (2-4), 91–133. https://doi.org/10.1016/S0341-8162(02)00143-1.
Polyakov, V.O., Nichols, M.H., McClaran, M.P., Nearing, M.A., 2014. Effect of check dams on runoff, sediment yield, and retention on small semiarid watersheds. J. Soil Water Conserv. 69 (5), 414–421. https://doi.org/10.2489/jswc.69.5.414.
Pulido, M., Schnabel, S., Lavado Contador, J.F., Lozano-Parra, J., González, F., 2018. The impact of heavy grazing on soil quality and pasture production in rangelands of SW Spain. Land Degrad. Dev. 29 (2), 219–230. https://doi.org/10.1002/ldr.2501.
Quiñonero-Rubio, J., Boix-Fayos, C., de Vente, J., 2013. Desarrollo y aplicación de un índice multifactorial de conectividad de sedimentos a escala de Cuenca. Cuadernos de investigación geográfica/Geographical Research Letters 203–223. https://doi.org/10.1016/10.18172/cig.1988.
Quiñonero-Rubio, J.M., Nadeu, E., Boix-Fayos, C., de Vente, J., 2016. Evaluation of the effectiveness of forest restoration and check-dams to reduce catchment sediment yield. Land Degrad. Dev. 27 (4), 1018–1031. https://doi.org/10.1002/ldr.2331.
Ran, D.-C., Luo, Q.-H., Zhou, Z.-H., Wang, G.-Q., Zhang, X.-H., 2008. Sediment retention by check dams in the Hekouzhen-Longmen Section of the Yellow River. Int. J. Sedim. Res. 23 (2), 159–166. https://doi.org/10.1016/S1001-6279(08)60015-3.
Riverscapes-Consortium, 2018. Geomorphic Change Detection Software.
Rubio-Delgado, J., Guillén, J., Corbacho, J., Gómez-Gutiérrez, Á., Baeza, A., Schnabel, S., 2017. Comparison of two methodologies used to estimate erosion rates in Mediterranean ecosystems: 137Cs and exposed tree roots. Sci. Total Environ. 605, 541–550. https://doi.org/10.1016/j.scitotenv.2017.06.248.
Rubio-Delgado, J., Schnabel, S., Gómez-Gutiérrez, Á., Sánchez-Fernández, M., 2018. Estimation of soil erosion rates in dehesas using the inflection point of holm oaks. Catena 166, 56–67. https://doi.org/10.1016/j.catena.2018.03.017.
Schnabel, S., 1997. Soil erosion and runoff production in a small watershed under silvo-pastoral landuse (dehesas) in Extremadura. Geoforma Ediciones, Spain.
Schnabel, S., Ceballos Barbancho, A., Gómez-Gutiérrez, Á., 2010. Erosión hídrica en la dehesa extremeña. in: Schnabel, S.L.C., J.F.; Gómez-Gutiérrez A.; García Marín, R (Ed.), Aportaciones a la geografía física de extremadura con especial referencia a las Dehesas, pp. 153-185.
Schnabel, S., Gómez-Gutiérrez, Á., 2013. The role of interannual rainfall variability on runoff generation in a small dry sub-humid watershed with disperse tree cover. Cuadernos de Investigación Geográfica 39, 259–285. https://doi.org/10.1016/10.18172/cig.1991.
Schnabel, S., Dahlgren, R.A., Moreno-Marcos, G., 2013. Soil and water dynamics. In: Campos, P., Oviedo, J.S., Díaz, M., Montero, G. (Eds.), Mediterranean oak woodland working landscapes. Springer, pp. 91–121.
Schnabel, S., Lozano-Parra, J., Gómez-Gutiérrez, Á., Alfonso-Torreño, A., 2018. Hydrological dynamics in a small catchment with silvopastoral land use in SW Spain. Cuadernos de Investigación Geográfica 44, 557–580. https://doi.org/10.1016/10.18172/cig.3378.
Sidle, R.C., Gomi, T., Usuga, J.C.L., Jarihani, B., 2017. Hydrogeomorphic processes and scaling issues in the continuum from soil pedons to catchments. Earth Sci. Rev. 175, 75–96. https://doi.org/10.1016/j.earscirev.2017.10.010.
Sidle, R.C., Jarihani, B., Kaka, S.I., Koci, J., Al-Shaibani, A., 2019. Hydrogeomorphic processes affecting dryland gully erosion: Implications for modelling. Progress in Physical Geography: Earth and Environment 43 (1), 46–64. https://doi.org/10.1177/0309133318819403.
Sidle, R.C., Sasaki, S., Otsuki, M., Noguchi, S., Rahim Nik, A., 2004. Sediment pathways in a tropical forest: effects of logging roads and skid trails. Hydrol. Process. 18 (4), 703–720. https://doi.org/10.1002/hyp.1364.
Sidle, R.C., Ziegler, A.D., 2010. Elephant trail runoff and sediment dynamics in northern Thailand. J. Environ. Qual. 39 (3), 871–881. https://doi.org/10.2134/jeq2009.0218.
Sidle, R.C., Ziegler, A.D., Negishi, J.N., Nik, A.R., Siew, R., Turkelboom, F., 2006. Erosion processes in steep terrain—truths, myths, and uncertainties related to forest management in Southeast Asia. For. Ecol. Manage. 224 (1-2), 199–225. https://doi.org/10.1016/j.foreco.2005.12.019.
Talema, A., Poesen, J., Muys, B., Padro, R., Dibaba, H., Diels, J., 2019. Survival and growth analysis of multipurpose trees, shrubs, and grasses used to rehabilitate badlands in the subhumid tropics. Land Degrad. Dev. 30, 470–480. https://doi.org/10.1002/ldr.3239.
Tang, H., Pan, H., Ran., Q., 2020. Impacts of filled check dams with different deployment strategies on the flood and sediment transport processes in a Loess Plateau catchment. Water, 12, 1319. https://doi.org/10.3390/w12051319.
Tarboton, D.G., Dash, P., Sazib, N., 2015. TauDEM, Terrain analysis using digital elevation models.
Taye, G., Poesen, J., Vanmaercke, M., van Wesemael, B., Martens, L., Teka, D., Nyssen, J., Deckers, J., Vanacker, V., Haregeweyn, N., Hallet, V., 2015. Evolution of the effectiveness of stone bunds and trenches in reducing runoff and soil loss in the semi-arid Ethiopian highlands. Zeitschrift für Geomorphologie 59 (4), 477–493. https://doi.org/10.1127/zfg/2015/0166.
Turner, D., Lucieer, A., De Jong, S.M., 2015. Time series analysis of landslide dynamics using an unmanned aerial vehicle (UAV). Remote Sensing 7, 1736–1757. https://doi.org/10.3390/rs70201736.
Vaezi, A.R., Abbasi, M., Keesstra, S., Cerdà, A., 2017. Assessment of soil particle erodibility and sediment trapping using check dams in small semi-arid catchments. Catena 157, 227–240. https://doi.org/10.1016/j.catena.2017.05.021.
van der Waal, B., Rowntree, K., 2018. Landscape connectivity in the upper Mzimvubu river catchment: an assessment of anthropogenic influences on sediment connectivity. Land Degrad. Dev. 29 (3), 713–723. https://doi.org/10.1002/ldr.2766.
Vanmaercke, M., Poesen, J., Verstraeten, G., de Vente, J., Ocakoglu, F., 2011. Sediment yield in Europe: spatial patterns and scale dependency. Geomorphology 130 (3-4), 142–161. https://doi.org/10.1016/j.geomorph.2011.03.010.
Waterhouse, J., Schaffelke, B., Bartley, R., Eberhard, R., Brodie, J., Star, M., Thorburn, P., Rolfe, J., Ronan, M., Taylor, B., 2017. Scientific Consensus Statement: Land Use Impacts on Great Barrier Reef Water Quality and Ecosystem Condition (Queensland Government, 2017). chapter 5: Overview of Key Findings, Management Implications and Knowledge Gaps, 15.
Wheaton, J.M., Brasington, J., Darby, S.E., Sear, D.A., 2010. Accounting for uncertainty in DEMs from repeat topographic surveys: improved sediment budgets. Earth Surf. Proc. Land. 35, 136–156. https://doi.org/10.1002/esp.1886.
Wester, T., Wasklewicz, T., Staley, D., 2014. Functional and structural connectivity within a recently burned drainage basin. Geomorphology 206, 362–373. https://doi.org/10.1016/j.geomorph.2013.10.011.
Wilkinson, S.N., Kinsey-Henderson, A.E., Hawdon, A.A., Hairsine, P.B., Bartley, R., Baker, B., 2018. Grazing impacts on gully dynamics indicate approaches for gully erosion control in northeast Australia. Earth Surf. Proc. Land. 43 (8), 1711–1725. https://doi.org/10.1002/esp.4339.
Wohl, E., Magilligan, F.J., Rathburn, S.L., 2017. Introduction to the special issue: Connectivity in Geomorphology. Geomorphology 277, 1–5. https://doi.org/10.1016/j.geomorph.2016.11.005.
Woodget, A.S., Carbonneau, P.E., Visser, F., Maddock, I.P., 2015. Quantifying submerged fluvial topography using hyperspatial resolution UAS imagery and structure from motion photogrammetry. Earth Surf. Proc. Land. 40 (1), 47–64. https://doi.org/10.1002/esp.3613.
Xu, Y., Fu, B., He, C., 2013. Assessing the hydrological effect of the check dams in the Loess Plateau, China, by model simulations. Hydrol. Earth Syst. Sci. 17, 2185–2193. https://doi.org/10.5194/hess-17-2185-2013.
Zhang, X., She, D., Hou, M., Wang, G., Liu, Y.i., 2021. Understanding the influencing factors (precipitation variation, land use changes and check dams) and mechanisms controlling changes in the sediment load of a typical Loess watershed. China. Ecological Engineering 163, 106198. https://doi.org/10.1016/j.ecoleng.2021.106198.
Zhao, Y., Jia, R.L., Wang, J., 2019. Towards stopping land degradation in drylands: Water-saving techniques for cultivating biocrusts in situ. Land Degrad. Dev. 30 (18), 2336–2346. https://doi.org/10.1002/ldr.3423.